On the analytical approach to the linear analysis of an arbitrarily curved spatial Bernoulli-Euler beam

G. Radenković[1,2], A. Borković[2*]

[1]Faculty of Civil Engineering, University of Belgrade, Bulevar kralja Aleksandra 73, 11000 Belgrade, Serbia

[2]University of Banja Luka, Faculty of Architecture, Civil Engineering and Geodesy, Department of Mechanics and Theory of Structures, 78000 Banja Luka, Bosnia and Herzegovina, aleksandar.borkovic@aggf.unibl.org

Abstract:

The equilibrium and kinematic equations of an arbitrarily curved spatial Bernoulli-Euler beam are derived with respect to a parametric coordinate and compared with those of the Timoshenko beam. It is shown that the beam analogy follows from the fact that the left-hand side in all the four sets of those equations are the covariant derivatives of unknown vector. Furthermore, an elegant primal form of the equilibrium equations is composed. No additional assumptions, besides those of the linear Bernoulli-Euler theory, are introduced, which makes the theory ideally suited for the analytical assessment of big-curvature beams. The curvature change is derived with respect to both convective and material/spatial coordinates, and some aspects of its definition are discussed. Additionally, the stiffness matrix of an arbitrarily curved spatial beam is calculated with the flexibility approach utilizing the relative coordinate system. The numerical analysis of the carefully selected set of examples proved that the present analytical formulation can deliver valid benchmark results for testing of the purely numeric methods.

Keywords: curved spatial beam, beam equations, analytical solution, parametric coordinate, curvature change, big-curvature beam

1. Introduction

The present-day engineering is facing a growing need for the development of novel types of cost-effective structures which are simultaneously resistant and flexible. Indispensable components of these structures are curved spatial beams, and their application is fundamental in various fields of engineering. Although there is a vast amount of research devoted to the beam modeling, the exponential progress of software and hardware capabilities enables the development of more accurate advanced mathematical and mechanical models. The rigorous analysis of arbitrarily curved spatial beams is often disregarded due to the difficulties which are inherent in the modeling of these types of structures. The non-unit tangential base vector of an arbitrary parametric curve returns the nonconstant determinant of metric tensor g_{ij} of the beam axis. Furthermore, the initial curvature correction term g_0, which relates the base vector at an arbitrary point of a cross section with the base vector at the centroid, complicates the problem. These two quantities are often approximated in various ways in order to calculate the response of a curved spatial beam.

Plane circular beams are readily classified as *small-*, *medium-* and *big-curvature* beams, depending on the value Kh where K is the curvature of the beam axis while h is the height of a cross section, [1]. For spatial beams with variable curvature, this definition is more complex. One option is to use the value $K_{max}h_{max}$, where K_{max} is the maximum value of the curvature of the beam axis while h_{max} is the maximum dimension of the cross section in the planes parallel to the osculating plane at the position of K_{max}, [2]. In this way, $K_{max}h_{max}\in(0,2)$ and it is referred here to as the (*maximum local*) *curviness* of a beam. Thus, the term *arbitrarily curved* does not refer just to the shape of the beam axis and twist of the cross section, but, more importantly, to its curviness $K_{max}h_{max}$. Although the strict limits do not exist, [1], we will say that the beam has small curvature if its curviness is $K_{max}h_{max}<0.01$, while it has medium curvature if $0.01\leq K_{max}h_{max}<0.1$. All the other cases belong to the category of big-curvature beams. The

lack of benchmark test results for the recent developments of big-curvature beam model in the frame of isogeometric analysis (IGA), [2], [3], [4], and [5], was one of the main motives for the present research.

Next, the main contributions to the analytical assessment of spatially curved beams are summarized. The first beam theories are developed by Bernoulli and Euler, and later generalized by Kirchhoff, Clebsch, and Love, [6]. Ericksen and Truesdell precisely defined the beam strain and stress, [7], while Washizu gave a significant contribution to the analytical approach for naturally curved and twisted slender beams with warping effect in the context of the small-curvature theory, [8]. Influence of the extensibility of the beam axis is analyzed in [9] and compared with Lamb's inextensional theory. The authors start from the model of big-curvature beams but simplify afterward due to the inherent complexity of the obtained expressions. Similar approximations are often encountered in the literature and justified by the small influence of the higher order terms present in the beam metric.

The geometry of small strains is analogous to the equilibrium of internal forces which leads to the conjugate beam theory. For small-curvature beams, the conjugate beam analogy is generalized in [10] and [11], and extended for the curved bar resting on an external medium in [12]. The general solution to the system of beam equations with respect to the Frenet-Serret (FS) frame of reference can be found in [13] and [14]. An analytical study of small-curvature spatial arches defined in global coordinates is presented in [15], with examples employing only constant curvature. The authors extended their approach to non-naturally curved beams by scaling of the non-unitary tangential base vector, [16], and emphasized the lower triangular nature of the system of beam equations which enables a successive integration, [17].

A closed-form solution for the static response of the big-curvature in-plane beams is derived in [18]. The authors extended their approach to shear deformable [19] and composite beams [20] where the scalar function $1/g_0$ is approximated with the second-order Taylor polynomial which is known as the Lure-type approximation, [21].

The asymptotic modeling of small-curvature elastic rods has attracted a lot of attention. This method is based on an idea to approximate the beam solution with a formal expansion in power series in terms of a small parameter (diameter of the cross section), [22]. The standard assumptions of the beam theories are not required since they follow as the necessary and sufficient conditions for the convergence of results in this approach, [22]. The theory is further refined in [23], [24], and [25], while the restriction of the inextensible axis is applied in [26] utilizing the parametric coordinate.

Many researchers focus on the derivation of the stiffness matrix solely, while the analytical solution is utilized for the determination of the accurate nodal values and/or appropriate basis functions. The stiffness coefficients for a set of in-plane thin curved beams are readily derived, [27]. By employing the Lure-type approximation of $1/g_0$, the hybrid approach is successfully applied for C^0 curved beam element in [28]. A similar formulation is developed in [29] where the beam axis is described with cubic B-spline while a general format for the stiffness matrix of curved beams based on the three independent equilibrium states is presented in [30]. Furthermore, the derivation of the stiffness matrix using the exponential basis functions which satisfy the homogeneous part of the differential equation of a beam is viable, [31]. This approach alleviates the shear and membrane locking for beams with small curvature. The application of the basis functions which are based on real deformations significantly improves the accuracy, [32]. The exact stiffness matrix and nodal force vector of arbitrarily curved plane beams are discussed in [33] using the Lure-type approximation. Finally, the straightforward approach for the derivation of the stiffness matrix by the successive imposition of all generalized unit displacements is given in [34] and [35].

Although the analytical studies of curved beams are frequent in literature, the general approach to the linear static analysis of arbitrarily curved spatial beams does not exist. The beam equations are readily derived with respect to the FS frame of reference while making additional assumptions regarding

the beam metric. Here, an arbitrary parametric coordinate is consistently utilized for the modeling of a big-curvature Bernoulli-Euler (BE) beam and the complete metric is employed. The parametric coordinate is already indirectly applied by the transformation of the FS expressions in [16]. Here, it is explicitly shown that the arc-length form of beam equations follows as a special case of the general parametric equations. Additionally, the curvature change with respect to the FS coordinate system is discussed and derived in two ways: by assigning the convective property to the arc-length coordinate and by the linearization of spatial configuration with respect to the material configuration.

An elegant procedure for the derivation of the stiffness matrix via flexibility approach is introduced. This matrix is extensively compared with the one obtained using the weak form of equilibrium, where the exact basis functions are derived from the analytical solution of the beam equations. These functions are cumbersome and their utilization is not efficient for every-day use. Nevertheless, the exact basis functions should be viewed as an important guide when choosing suitable approximative functions for numerical analysis, especially if the accuracy is of the primary interest, [32].

All these considerations are related to the big-curvature beam model, where no higher-order terms of the beam metric are neglected. These models are rarely examined within the analytic context and a few isogeometric numeric approaches have emerged lately, [2], [3], and [5]. Generally, IGA enables the high-accuracy calculation of curved beams and analytical results can serve for preliminary validation of these formulations, [36], [37], [38], [39], [40], [41]. Therefore, the accuracy and limits of the applicability of the analytic approach for linear analysis of the BE beam model without warping are investigated here.

The paper is organized as follows. The next section gives some basics of the beam metric. The third section represents the core of the research where the beam equations are derived strictly and their solution is discussed. It is followed by the procedure for the derivation of the stiffness matrix and numerical applications. Concise conclusions and directions for further research are given in the last section. Some remarks regarding the Christoffel symbols, the change of curvature, and closed-form expressions are given in Appendices.

2. Metric of the spatial beam

Basic relations of beam metric are briefly presented in this section. Tensor calculus is employed and standard notation for covariance and contravariance of components is utilized via lower and upper indices, respectively. The analogous convention is used for the designation of the base vectors which constitute the original basis and its reciprocal counterpart. For a more thorough treatment, the paper [2] is recommended.

The classic BE assumption that a beam cross section is rigid and perpendicular to the deformed beam axis is enforced. Let us note three different frames of reference in Fig. 1. The first one is the FS frame defined with axes (s, α, β) and unit base vectors ($\mathbf{t}$, $\mathbf{n}$, $\mathbf{b}$). This is the intrinsic frame of the beam axis and it must be considered directly or referred to while using some alternative coordinate system. Note that $s \in [0, L]$, where L is the length of the beam. The second frame, (s, η, ζ) keeps the arc-length coordinate s, but the two other coordinate lines are here aligned with the principal axes of the second moment of area of a cross section at the centroid and their unit base vectors are ($\mathbf{t}$, $\mathbf{g}_2$, $\mathbf{g}_3$). Observe that both ($\mathbf{n}$, $\mathbf{b}$) and ($\mathbf{g}_2$, $\mathbf{g}_3$) belong to the normal plane of the beam axis and they make an arbitrary initial angle θ, Fig. 1. Finally, the third frame of reference (ξ, η, ζ) with base vectors ($\mathbf{g}_1$, $\mathbf{g}_2$, $\mathbf{g}_3$) is utilized. This frame adopts an arbitrary parameterization of the beam axis where the intensity of $\mathbf{g}_1$ varies along the coordinate line ξ, Fig. 1. The domain of this coordinate depends on the adopted parameterization. Since the arc-length parameterization exists only for a handful of curves, an arbitrary parametrization is necessary and it is utilized here primarily. Due to the BE hypothesis, the complete kinematics of the

beam is defined from translations of the beam axis and rotation of a cross section around the $\mathbf{g}_1$ basis (angle of twist).

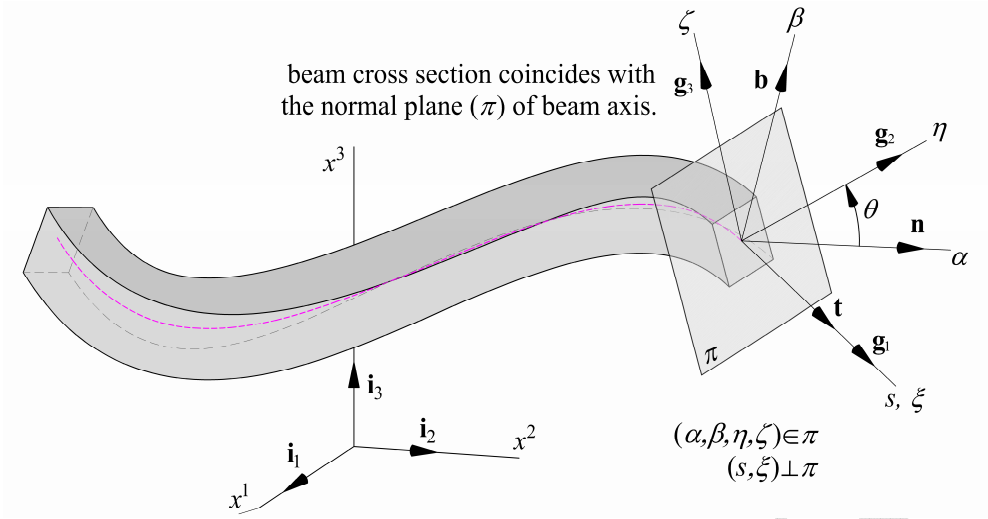

Fig. 1. An arbitrarily curved spatial BE beam. Coordinate systems.

The position vector of the beam axis is $\mathbf{r}=\mathbf{r}(\xi)$ while its global rectangular Cartesian components are $x_m(\xi)=x^m(\xi)$, where m=1,2,3. The derivatives of this vector with respect to the s and ξ coordinates return the base vectors $\mathbf{t}$ and $\mathbf{g}_1$:

$$\mathbf{r}=x^m\,\mathbf{i}_m,\quad \mathbf{t}=\frac{\mathrm{d}\mathbf{r}}{\mathrm{d}s},\quad \mathbf{g}_1=\mathbf{r}_{,1}=\frac{\mathrm{d}\mathbf{r}}{\mathrm{d}\xi}=x^m_{,1}\,\mathbf{i}_m=\frac{\mathrm{d}\mathbf{r}}{\mathrm{d}s}\frac{\mathrm{d}s}{\mathrm{d}\xi}=\sqrt{x^m_{,1}x_{m,1}}\,\mathbf{t}, \tag{1}$$

where $\mathbf{i}_m=\mathbf{i}^m$ are the base vectors of the Cartesian coordinate system while the partial derivative with respect to the k^{th} coordinate of the (ξ, η, ζ) system is designated with $(\cdot)_{,k}$. The other two base vectors of (ξ, η, ζ) system are:

$$\mathbf{g}_2=\mathbf{r}_{,2}=x^n_{,2}\,\mathbf{i}_n,\quad \mathbf{g}_3=\mathbf{r}_{,3}=x^n_{,3}\,\mathbf{i}_n, \tag{2}$$

and they are calculated via rotation of the normal and binormal, [2].

The squares of the arc-length and parametric coordinates are related via the determinant of the metric tensor:

$$g_{ij}=\begin{bmatrix} g_{11} & 0 & 0\\ 0 & 1 & 0\\ 0 & 0 & 1\end{bmatrix},\quad g_{11}=\mathbf{g}_1\cdot\mathbf{g}_1=x^m_{,1}x_{m,1},\qquad g=\det(g_{ij})=g_{11},\quad g^{11}=\frac{1}{g_{11}},$$
$$ds^2=\mathrm{d}x^m\mathrm{d}x_m=g\mathrm{d}\xi^2\quad\Rightarrow\quad \mathrm{d}s=\sqrt{g}\,\mathrm{d}\xi. \tag{3}$$

Observe the relation between the Cartesian components of the base vectors ($\mathbf{g}_1$, $\mathbf{g}_2$, $\mathbf{g}_3$) and their reciprocal counterparts ($\mathbf{g}^1$, $\mathbf{g}^2$, $\mathbf{g}^3$):

$$x^{,1}_i=\frac{1}{g}x_{i,1},\quad x^{,2}_i=x_{i,2},\quad x^{,3}_i=x_{i,3}. \tag{4}$$

Covariant components of the curvature vector with respect to the (ξ, η, ζ) system are:

$$K_1=\sqrt{g}\tau+\theta_{,1},\quad K_2=K\sin\theta,\quad K_3=K\cos\theta, \tag{5}$$

where K and τ are the curvature and torsion of the beam axis with respect to the FS frame of reference, respectively.

The Christoffel symbols of the second kind associate the partial derivative of base vectors with the same set of these vectors:

$$\mathbf{g}_{i,j} = \Gamma_{ij}^{k}\mathbf{g}_k, \tag{6}$$

and they are often represented in matrix form, [2]:

$$\begin{bmatrix}\mathbf{g}_{1,1}\\ \mathbf{g}_{2,1}\\ \mathbf{g}_{3,1}\end{bmatrix} = \begin{bmatrix}\Gamma_{11}^{1} & gK_3 & -gK_2\\ -K_3 & 0 & K_1\\ K_2 & -K_1 & 0\end{bmatrix}\begin{bmatrix}\mathbf{g}_1\\ \mathbf{g}_2\\ \mathbf{g}_3\end{bmatrix}. \tag{7}$$

The fact that the Christoffel symbols of the second kind are not tensors is discussed in the Appendix A.

3. Equations of an arbitrary curved BE beam

In this section, the BE beam equations are derived and comparison with the Timoshenko theory is remarked. It proves that the distinction between the equations of these two theories exists only in stress-strain relations and in displacement-rotation equations.

3.1 Equilibrium equations

The equations of equilibrium of spatial beam are often expressed with respect to the arc-length coordinate, e.g. [13]. These equations are here concisely derived with respect to an arbitrary parametric coordinate. They are valid for both the BE and Timoshenko beam models.

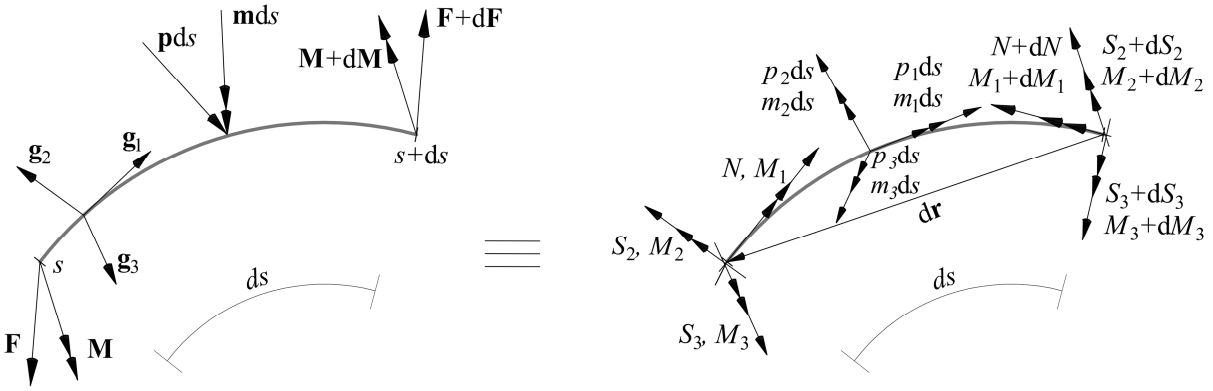

Fig. 2. Differential element of a spatial beam and stress resultants

The requirement for force equilibrium of the differential element in Fig. 2 gives:

$$\mathrm{d}\mathbf{F} = \mathbf{p}\mathrm{d}s, \tag{8}$$

which can be written as:

$$\frac{\mathrm{d}\mathbf{F}}{\mathrm{d}\xi} = \sqrt{g}\mathbf{p} \Rightarrow F_{k|1}\mathbf{g}^k = \sqrt{g}\,p_k\mathbf{g}^k \Rightarrow F_{k|1} = \sqrt{g}\,p_k, \tag{9}$$

where $(.)_{|1}$ stands for the covariant derivative with respect to the parametric coordinate ξ.

Similarly, the requirement for moment equilibrium of the differential element in Fig. 2 gives:

$$\mathrm{d}\mathbf{M} + \mathrm{d}\mathbf{r}\times\mathbf{F} = \mathbf{m}\mathrm{d}s, \tag{10}$$

which, using d**r**=**t**ds, can be written as:

$$\frac{\mathrm{d}\mathbf{M}}{\mathrm{d}\xi} = \sqrt{g}(\mathbf{m} - \mathbf{t}\times\mathbf{F}) \Rightarrow M_{k|1}\mathbf{g}^k = \sqrt{g}(m_k - e_{1mk}F^m)\mathbf{g}^k \Rightarrow M_{k|1} = \sqrt{g}(m_k - e_{1mk}F^m), \tag{11}$$

where e_{ijk} is the permutation symbol.

In this way, the equations of equilibrium are valid for an arbitrary parametric coordinate. For g=1, these equations reduce to the ones derived with respect to the arc-length coordinate. Following the vectors of stress resultants **F**, stress couples **M**, external forces **p** and moments **m**, and differential of position vector d**r** are introduced in the previous equations:

$$\begin{aligned}&\mathbf{F}^{\mathrm{T}}=\begin{bmatrix}F_1 & F_2 & F_3\end{bmatrix}=\begin{bmatrix}N & S_2 & S_3\end{bmatrix},\quad \mathbf{M}^{\mathrm{T}}=\begin{bmatrix}M_1 & M_2 & M_3\end{bmatrix},\\&\mathbf{p}^{\mathrm{T}}=\begin{bmatrix}p_1 & p_2 & p_3\end{bmatrix},\quad \mathbf{m}^{\mathrm{T}}=\begin{bmatrix}m_1 & m_2 & m_3\end{bmatrix},\quad \mathrm{d}\mathbf{r}^{\mathrm{T}}=\begin{bmatrix}\mathrm{d}r_1 & \mathrm{d}r_2 & \mathrm{d}r_3\end{bmatrix}.\end{aligned} \tag{12}$$

3.2 Stress-strain relations

After the calculation of the section forces, an appropriate constitutive relation should be postulated in order to obtain the flexural, torsional and axial strains of the BE beam axis. The Timoshenko model is omitted, but it would require the calculation of the shear strains of the beam axis, as well. For a big-curvature BE beam, this relation is rigorously derived in [2] from the principle of virtual work by imposing the convective property to the parametric coordinate ξ. In this way, the energetically conjugated section forces are related to the reference strains of the beam axis (axial strain and three components of the curvature change: ε_{11}, κ_1, κ_2, and κ_3):

$$\begin{aligned}&\bar{\mathbf{R}}=\bar{\mathbf{D}}\boldsymbol{\varepsilon}\Rightarrow\boldsymbol{\varepsilon}=\bar{\mathbf{D}}^{-1}\bar{\mathbf{R}},\\&\bar{\mathbf{R}}=\begin{bmatrix}\bar{N}\\ \bar{M}_1\\ \bar{M}_2\\ \bar{M}_3\end{bmatrix},\quad \bar{\mathbf{D}}=\frac{E}{g^2}\begin{bmatrix}A & 0 & I_2 & -I_3\\ 0 & gGI_{11}/\mathrm{E} & 0 & 0\\ I_2 & 0 & I_{22} & -I_{23}\\ -I_3 & 0 & -I_{32} & I_{33}\end{bmatrix},\quad \boldsymbol{\varepsilon}=\begin{bmatrix}\varepsilon_{11}\\ \kappa_1\\ \kappa_2\\ \kappa_3\end{bmatrix}=\begin{bmatrix}(g_{11}^{*}-g_{11})/2\\ K_1^{*}-K_1\\ \bar{K}_2^{*}-\bar{K}_2\\ \bar{K}_3^{*}-\bar{K}\end{bmatrix},\end{aligned} \tag{13}$$

where the asterisk denotes quantities in the deformed configuration. The geometric properties are:

$$\begin{aligned}&A=\int_A\frac{\left(1+\eta K_3-\zeta K_2\right)^2}{g_0}d\eta d\zeta,\quad I_2=\int_A\zeta\frac{1+\eta K_3-\zeta K_2}{g_0}d\eta d\zeta,\quad I_3=\int_A\eta\frac{1+\eta K_3-\zeta K_2}{g_0}d\eta d\zeta,\\&I_{23}=I_{32}=\int_A\frac{\eta\zeta}{g_0}d\eta d\zeta,\quad I_{22}=\int_A\frac{\zeta^2}{g_0}d\eta d\zeta,\quad I_{33}=\int_A\frac{\eta^2}{g_0}d\eta d\zeta,\quad I_{11}=\int_A\frac{1}{g_0}\left(\eta^2+\zeta^2\right)d\eta d\zeta,\end{aligned} \tag{14}$$

while E and G are Young's and shear moduli, respectively. The initial curvature correction term is defined as:

$$g_0=1-\eta K_3+\zeta K_2, \tag{15}$$

and it is frequently approximated in the existing literature, e.g. [28]. Here, following the approach given in [2, 3], the integrals in Eq. (14) are calculated analytically. Since the energetically conjugated forces are related to the standard section forces as:

$$\bar{N}=N-K_2M_2-K_3M_3,\quad \bar{M}_1=M_1,\quad \bar{M}_2=M_2,\quad \bar{M}_3=M_3, \tag{16}$$

the reference strains follow from the known stress resultant and stress couples. Note that the property I_{11} requires the torsional correction factor since Eq. (14) is valid only for circular cross sections, [2].

The other approach considered here is the simplest type of the small-curvature theory where the constitutive relations are the same as those for a straight beam. In this approach, there is no coupling of axial and bending actions, i.e. the matrix $\bar{\mathbf{D}}$ is diagonal with the standard geometric properties: area, torsion constant, and axial moments of inertia of cross section.

3.3 Kinematic equations

The next set of beam equations postulate relations between the reference strains and kinematic quantities.

3.3.1 Displacement equations

The convective property is not required for the following formulae. The first expression relates the displacement gradient and the axial strain of the beam axis:

$$u_{1|1} = \varepsilon_{11}, \tag{17}$$

and it is valid for both beam theories. For the BE model, the components of infinitesimal rotation, φ_2 and φ_3, are the gradients of the displacement of the beam axis:

$$u_{2|1} = \sqrt{g}\varphi_3, \quad u_{3|1} = -\sqrt{g}\varphi_2. \tag{18}$$

For the Timoshenko theory, these components are independent quantities:

$$u_{2|1} = \sqrt{g}\varphi_3 + \gamma_{12}, \quad u_{3|1} = -(\sqrt{g}\varphi_2 - \gamma_{13}), \tag{19}$$

where γ_{12} and γ_{13} are shear strains of the beam axis.

3.3.2 Rotation-strain relations

Starting from the linearized expressions derived in [2]:

$$\begin{aligned}
\kappa_1 &= K_1^* - K_1 \approx K_2\left(\mathbf{g}_2 \cdot \mathbf{u}_{,1}\right) + K_3\left(\mathbf{g}_3 \cdot \mathbf{u}_{,1}\right) + \hat{\varphi}^1_{,1}, \\
\kappa_2 &= g^* K_2^* - gK_2 \approx -\mathbf{g}_3 \cdot \left(\mathbf{u}_{,11} - \Gamma^1_{11}\mathbf{u}_{,1}\right) + gK_3\hat{\varphi}^1, \\
\kappa_3 &= g^* K_3^* - gK_3 \approx \mathbf{g}_2 \cdot \left(\mathbf{u}_{,11} - \Gamma^1_{11}\mathbf{u}_{,1}\right) - gK_2\hat{\varphi}^1,
\end{aligned} \tag{20}$$

we can obtain a relation between the curvature change and infinitesimal rotation. Here, $\hat{\varphi}^1 = \varphi_1 / \sqrt{g}$ is the physical component of the angle of twist as a function of parameter ξ. For κ_3 we found that:

$$\begin{aligned}
\kappa_3 &= \left(\mathbf{g}_2 \cdot \mathbf{u}_{,1}\right)_{,1} - \mathbf{g}_{2,1} \cdot \mathbf{u}_{,1} - \Gamma^1_{11}\mathbf{g}_2 \cdot \mathbf{u}_{,1} - gK_2\hat{\varphi}^1 = \left(\hat{\mathbf{u}}_{2|1}\right)_{,1} - \left(-K_3\mathbf{g}_1 + K_1\mathbf{g}_3\right) \cdot \mathbf{u}_{,1} - \Gamma^1_{11}\hat{\mathbf{u}}_{2|1} - gK_2\hat{\varphi}^1 = \\
&= \left(\sqrt{g}\varphi_3\right)_{,1} + K_3\hat{\mathbf{u}}_{1|1} - K_1\hat{\mathbf{u}}_{3|1} - \Gamma^1_{11}\hat{\mathbf{u}}_{2|1} - gK_2\hat{\varphi}^1 = \\
&= \sqrt{g}\varphi_{3,1} + \sqrt{g}\Gamma^1_{11}\varphi_3 + K_3\varepsilon_{11} + \sqrt{g}K_1\varphi_2 - \sqrt{g}\Gamma^1_{11}\varphi_3 - gK_2\hat{\varphi}^1 = \\
&= \sqrt{g}\left(\varphi_{3,1} - K_2\varphi_1 + K_1\varphi_2\right) + K_3\varepsilon_{11} = \sqrt{g}\varphi_{3|1} + K_3\varepsilon_{11},
\end{aligned} \tag{21}$$

where $\hat{\mathbf{u}}_2$ and $\hat{\mathbf{u}}_3$ are displacement vectors along local (η, ζ) axes. A similar expression can be analogously derived for κ_2, while for κ_1 we can show that:

$$\begin{aligned}
\kappa_1 &= K_2\hat{\mathbf{u}}_{2|1} + K_3\hat{\mathbf{u}}_{3|1} + \hat{\varphi}^1_{,1} = K_2\sqrt{g}\varphi_3 - K_3\sqrt{g}\varphi_2 + \left(\frac{1}{\sqrt{g}}\varphi_1\right)_{,1} = \\
&= \frac{1}{\sqrt{g}}\varphi_{1,1} - \frac{1}{2}\frac{1}{g\sqrt{g}}g_{,1}\varphi_1 + \sqrt{g}K_2\varphi_3 - \sqrt{g}K_3\varphi_2 = \\
&= \frac{1}{\sqrt{g}}\left(\varphi_{1,1} - \Gamma^1_{11}\varphi_1 + gK_2\varphi_3 - gK_3\varphi_2\right) = \frac{1}{\sqrt{g}}\varphi_{1|1}.
\end{aligned} \tag{22}$$

To summarize, the rotation-strain relations are:

$$\varphi_{1|1}=\sqrt{g}\kappa_1,\quad \varphi_{2|1}=\frac{1}{\sqrt{g}}\left(\kappa_2-K_2\varepsilon_{11}\right),\quad \varphi_{3|1}=\frac{1}{\sqrt{g}}\left(\kappa_3-K_3\varepsilon_{11}\right), \tag{23}$$

and they are valid for the Timoshenko beam theory, as well. Additional considerations regarding the change of curvature with respect to the FS frame are given in the Appendices B and C.

3.4 Analogy of beam equations and their solution

Let us now observe the derived BE beam equations in compact form:

$$\begin{aligned}
&-\text{force equations:} && F_{k|1}=f_k^F,\quad \left(f_k^F=\sqrt{g}\,p_k\right),\\
&-\text{moment equations:} && M_{k|1}=f_k^M,\quad \left(f_k^M=\sqrt{g}\left(m_k-e_{1mk}F^m\right)\right),\\
&-\text{rotation equations:} && \varphi_{k|1}=f_k^\varphi,\quad \left(f_1^\varphi=\sqrt{g}\kappa_1,\ f_q^\varphi=\left(\kappa_q-K_q\varepsilon_{11}\right)/\sqrt{g},\ q=2,3\right),\\
&-\text{displacement equations:} && u_{k|1}=f_k^u,\quad \left(f_1^u=\varepsilon_{11},\ f_2^u=\sqrt{g}\varphi_3,\ f_3^u=-\sqrt{g}\varphi_2\right).
\end{aligned} \tag{24}$$

Evidently, the beam analogy follows from the fact that the left-hand side in all the four sets of equations are the covariant derivatives of the observed vector: section forces, section moments, infinitesimal rotations, and displacements. With appropriate boundary conditions, these equations can be solved successively, since solutions of one set represent constant terms in the next set.

The fundamental matrix of the homogeneous parts of Eq. (24) is actually the transpose of the Jacobian matrix of transformation between local (ξ, η, ζ) and global Cartesian coordinates x_m, $\mathbf{J}^{\mathrm{T}}$. Therefore, the elements of this matrix are actually the Cartesian components of the base vectors ($\mathbf{g}_1$, $\mathbf{g}_2$, $\mathbf{g}_3$) and its columns form three linearly independent solutions of the observed system. The Wronskian of this matrix is:

$$W(\xi)=\det\mathbf{J}^{\mathrm{T}}=\det\begin{bmatrix}\mathbf{g}_1\\ \mathbf{g}_2\\ \mathbf{g}_3\end{bmatrix}=\det\begin{bmatrix}x^1_{,1} & x^2_{,1} & x^3_{,1}\\ x^1_{,2} & x^2_{,2} & x^3_{,2}\\ x^1_{,3} & x^2_{,3} & x^3_{,3}\end{bmatrix}=\sqrt{g(\xi)}. \tag{25}$$

The particular solutions of the systems (24) are easily determined by the variation of constants and general solutions can be represented as:

$$\begin{aligned}
&F_k(\xi)=x^n_{,k}(\xi)\left[C_n^F+\int\frac{W_n^F(\xi)}{\sqrt{g(\xi)}}\mathrm{d}\xi\right],\quad M_k(\xi)=x^n_{,k}(\xi)\left[C_n^M+\int\frac{W_n^M(\xi)}{\sqrt{g(\xi)}}\mathrm{d}\xi\right],\\
&\varphi_k(\xi)=x^n_{,k}(\xi)\left[C_n^\varphi+\int\frac{W_n^\varphi(\xi)}{\sqrt{g(\xi)}}\mathrm{d}\xi\right],\quad u_k(\xi)=x^n_{,k}(\xi)\left[C_n^u+\int\frac{W_n^u(\xi)}{\sqrt{g(\xi)}}\mathrm{d}\xi\right],
\end{aligned} \tag{26}$$

where W_n^F, W_n^M, W_n^φ, and W_n^u are the Wronskians of the fundamental matrix with n^{th} column replaced with the values of constant terms $f_k^F, f_k^M, f_k^\varphi$, and f_k^u, respectively:

$$W_i^F=\sqrt{g}\,f_m^F x_i^{,m},\quad W_i^M=\sqrt{g}\,f_m^M x_i^{,m},\quad W_i^\varphi=\sqrt{g}\,f_m^\varphi x_i^{,m},\quad W_i^u=\sqrt{g}\,f_m^u x_i^{,m}, \tag{27}$$

which simplifies integrals in Eq. (26) to:

$$\begin{aligned}
&F_k(\xi)=x^n_{,k}(\xi)\left[C_n^F+\int f_m^F(\xi)x_n^{,m}(\xi)\mathrm{d}\xi\right],\quad M_k(\xi)=x^n_{,k}(\xi)\left[C_n^M+\int f_m^M(\xi)x_n^{,m}(\xi)\mathrm{d}\xi\right],\\
&\varphi_k(\xi)=x^n_{,k}(\xi)\left[C_n^\varphi+\int f_m^\varphi(\xi)x_n^{,m}(\xi)\mathrm{d}\xi\right],\quad u_k(\xi)=x^n_{,k}(\xi)\left[C_n^u+\int f_m^u(\xi)x_n^{,m}(\xi)\mathrm{d}\xi\right].
\end{aligned} \tag{28}$$

In order to obtain the constants of integration which have a clear physical interpretation, we can multiply these equations with $x_{i'}^{,j}$ and set $\xi=\xi_i$:

$$\begin{aligned} C_n^F(\xi_i) &= F_n^*(\xi_i) - \left(\int f_m^F(\xi) x_n^{,m}(\xi) \mathrm{d}\xi \right)\Big|_{\xi=\xi_i}, \quad C_n^M(\xi_i) = M_n^*(\xi_i) - \left(\int f_m^M(\xi) x_n^{,m}(\xi) \mathrm{d}\xi \right)\Big|_{\xi=\xi_i}, \\ C_n^\varphi(\xi_i) &= \varphi_n^*(\xi_i) - \left(\int f_m^\varphi(\xi) x_n^{,m}(\xi) \mathrm{d}\xi \right)\Big|_{\xi=\xi_i}, \quad C_n^u(\xi_i) = u_n^*(\xi_i) - \left(\int f_m^u(\xi) x_n^{,m}(\xi) \mathrm{d}\xi \right)\Big|_{\xi=\xi_i}, \end{aligned} \tag{29}$$

which returns the final form of these solutions:

$$\begin{aligned} F_k(\xi) &= x_{,k}^n(\xi) \left[F_n^*(\xi_i) + \int_{\xi_i}^{\xi} f_m^F(t) x_n^{,m}(t) dt \right], \; M_k(\xi) = x_{,k}^n(\xi) \left[M_n^*(\xi_i) + \int_{\xi_i}^{\xi} f_m^M(t) x_n^{,m}(t) dt \right], \\ \varphi_k(\xi) &= x_{,k}^n(\xi) \left[\varphi_n^*(\xi_i) + \int_{\xi_i}^{\xi} f_m^\varphi(t) x_n^{,m}(t) dt \right], \quad u_k(\xi) = x_{,k}^n(\xi) \left[u_n^*(\xi_i) + \int_{\xi_i}^{\xi} f_m^u(t) x_n^{,m}(t) dt \right]. \end{aligned} \tag{30}$$

The constants $F_n^*(\xi_i)$, $M_n^*(\xi_i)$, $\varphi_n^*(\xi_i)$, and $u_n^*(\xi_i)$, are now forces, moments, rotations, and displacements at the start of the beam *ik*, respectively. Importantly, the solution with respect to the arc-length coordinate follows as a special case for $g=1$.

Unfortunately, closed-form solutions of the integrals in these equations exist only for a few geometries. Therefore, some type of approximation must be introduced in order to obtain solutions.

3.5 The primal form of equilibrium equation

Let us derive the governing equations of the problem (24) with respect to the kinematic variables. From Eq. (11), shear forces are:

$$F_2 = m_3 - \frac{1}{\sqrt{g}} M_{3|1}, \quad F_3 = -m_2 + \frac{1}{\sqrt{g}} M_{2|1}, \tag{31}$$

which, using Eq. (16), reduces the number of equilibrium equations from six to four:

$$\begin{aligned} &\left(\bar{N} + K_2 M_2 + K_3 M_3 \right)_{|1} = \sqrt{g}\, p_1, \\ &M_{1|1} = \sqrt{g}\, m_1. \\ &M_{2|11} = g p_3 + \sqrt{g}\, m_{2|1}, \\ &M_{3|11} = -g p_2 + \sqrt{g}\, m_{3|1}. \end{aligned} \tag{32}$$

Substitution of equations (13), (23), (17), and (18) into (32) and some basic manipulations return:

$$\begin{aligned} &\left(T_1 u_{1|1} + T_3 u_{2|11} - T_2 u_{3|11} \right)_{|1} = \frac{g^{5/2}}{E} p_1, \\ &\left(I_{11} \varphi_{1|1} \right)_{|1} = \frac{g^2 m_1}{G}, \\ &\left(T_2 u_{1|1} - I_{23} u_{2|11} - I_{22} u_{3|11} \right)_{|11} = \frac{g^{5/2}}{E} \left(\sqrt{g}\, p_3 + m_{2|1} \right), \\ &\left(T_3 u_{1|1} + I_{23} u_{3|11} + I_{33} u_{2|11} \right)_{|11} = \frac{g^{5/2}}{E} \left(-\sqrt{g}\, p_2 + m_{3|1} \right), \end{aligned} \tag{33}$$

where:

$$
\begin{aligned}
T_1 &= A + 2I_2K_2 - 2I_3K_3 - 2I_{23}K_2K_3 + I_{22}K_2^{\,2} + I_{33}K_3^{\,2},\\
T_2 &= I_2 - I_{23}K_3 + I_{22}K_2,\\
T_3 &= -I_3 - I_{23}K_2 + I_{33}K_3.
\end{aligned}
\tag{34}
$$

Eq. (33) is a coupled system of linear differential equations where unknowns are covariant components of displacement of the beam axis and angle of twist of a cross section. Note that the coefficients of this system are functions of ξ, while:

$$
g_{\,|1} = 0, \quad K_{2|1} = K_{2,1}, \quad K_{3|1} = K_{3,1}. \tag{35}
$$

4. Basic flexibility method for numerical calculation of stiffness matrix

The procedure for an elegant derivation of the stiffness matrix of an arbitrarily curved spatial beam is briefly presented. The routine is general and applicable to all types of beams. The aim is to define the stiffness matrix **K** which relates the vectors of global nodal displacements **q** and vector of global external nodal loads **Q**, as **Kq=Q** where:

$$
\begin{aligned}
\mathbf{q}^{\mathrm{T}} &= \begin{bmatrix} u_i & v_i & w_i & \varphi_{xi} & \varphi_{yi} & \varphi_{zi} & u_k & v_k & w_k & \varphi_{xk} & \varphi_{yk} & \varphi_{zk} \end{bmatrix},\\
\mathbf{Q}^{\mathrm{T}} &= \begin{bmatrix} X_{ik} & Y_{ik} & Z_{ik} & M_{xik} & M_{yik} & M_{zik} & X_{ki} & Y_{ki} & Z_{ki} & M_{xki} & M_{yki} & M_{zki} \end{bmatrix}.
\end{aligned}
\tag{36}
$$

This is readily achieved by successive enforcement of 12 generalized unit displacements in order to determine 12x12=144 elements of the stiffness matrix, [34]. Here, we will derive the same matrix by calculating only 6x6=36 coefficients which are related to a carefully selected set of six independent kinematic quantities. The presented approach is similar to the one given in [33] for plane beams where the so-called force-transfer matrix is utilized, while the present procedure is based on the relative kinematics.

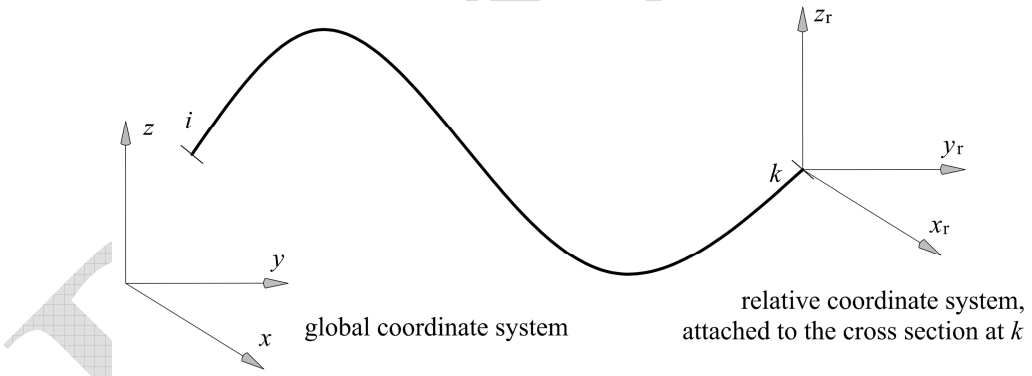

Fig. 3. Arbitrarily curved beam *ik*. Global and relative coordinate systems.

Let us observe the axis of an arbitrarily curved beam *ik* in Fig. 3 with the relative coordinate system (x_r, y_r, z_r) attached to the section *k*. The components of displacement and rotation at the section *i* with respect to this relative coordinate system are designated with u_{ji}^r and φ_{ji}^r, while these quantities for both sections with respect to the global coordinate system ($x=x^1$, $y=x^2$, $z=x^3$) are designated with u_{ji}, u_{jk}, φ_{ji}, and φ_{jk}. The present derivation is based on the relations between these components:

$$
u_{ji}^r = u_{ji} - u_{jk} - e_{jml}(x_k^m - x_i^m)\varphi_{lk}, \quad \varphi_{ji}^r = \varphi_{ji} - \varphi_{jk}, \quad j = x, y, z. \tag{37}
$$

Evidently, displacements and rotations of the section *k* with respect to the relative coordinate system are zero. Notice that u_{ji}^r and φ_{ji}^r represent six relative DOFs which are necessary and sufficient to describe

the complete stiffness matrix of the deformable beam *ik*. Equation (37) enables us to associate the absolute and relative kinematics of the beam end sections.

By utilizing this set of relative DOFs, we can derive the basic flexibility matrix (BFM) **d** which links the relative displacements at the section *i* with the section forces at the same section:

$$\begin{aligned}\boldsymbol{\Delta}^{\mathrm{T}} &= \left[u_{xi}^{r} \quad u_{yi}^{r} \quad u_{zi}^{r} \quad \varphi_{xi}^{r} \quad \varphi_{yi}^{r} \quad \varphi_{zi}^{r}\right],\\ \mathbf{S}^{\mathrm{T}} &= \left[X_{ik} \quad Y_{ik} \quad Z_{ik} \quad M_{xik} \quad M_{yik} \quad M_{zik}\right],\\ \boldsymbol{\Delta} &= \mathbf{dS}.\end{aligned} \tag{38}$$

This matrix can be derived by the standard unit force method where the section *k* should be viewed as fixed since we are determining the displacements and rotation components with respect to the relative coordinate system attached to this section. Depending on the adopted stress-strain relation, the BFM of appropriate beam model is obtained. For the big-curvature beams, special care must be paid to the energetically conjugated pairs of stress and strain, [2].

Because the BFM relates six independent kinematic quantities with six independent section forces, it has the inversion - the basic stiffness matrix $\mathbf{k}=\mathbf{d}^{-1}$. If we now introduce the relationship between the relative kinematics of the section *i* and global kinematics of the sections *i* and *k*:

$$\begin{aligned}&\boldsymbol{\Delta} = \mathbf{Hq}, \quad \mathbf{H} = \left[\mathbf{I}_{6\mathrm{x}6} \quad \mathbf{G}\right], \quad \mathbf{G} = \begin{bmatrix} -\mathbf{I}_{3\mathrm{x}3} & \mathbf{T} \\ \mathbf{0}_{3\mathrm{x}3} & -\mathbf{I}_{3\mathrm{x}3} \end{bmatrix},\\ &\mathbf{T} = \begin{bmatrix} 0 & (z_k - z_i) & -(y_k - y_i) \\ -(z_k - z_i) & 0 & (x_k - x_i) \\ (y_k - y_i) & -(x_k - x_i) & 0 \end{bmatrix},\end{aligned} \tag{39}$$

we can easily derive the global stiffness matrix **K** of an arbitrarily curved beam:

$$\mathbf{k\Delta} = \mathbf{S} \Rightarrow \mathbf{kHq} = \mathbf{S} \Rightarrow \mathbf{H}^{\mathrm{T}}\mathbf{kHq} = \mathbf{H}^{\mathrm{T}}\mathbf{S} \Rightarrow \mathbf{Kq} = \mathbf{Q}, \quad \left(\mathbf{H}^{\mathrm{T}}\mathbf{kH} = \mathbf{K}, \quad \mathbf{H}^{\mathrm{T}}\mathbf{S} = \mathbf{Q}\right). \tag{40}$$

Notice that the basic stiffness matrix is actually the first block of the global stiffness matrix **K**:

$$\mathbf{K} = \mathbf{H}^{\mathrm{T}}\mathbf{kH} = \begin{bmatrix} \mathbf{IkI} & \mathbf{IkG} \\ \mathbf{G}^{\mathrm{T}}\mathbf{kI} & \mathbf{G}^{\mathrm{T}}\mathbf{kG} \end{bmatrix} = \begin{bmatrix} \mathbf{k} & \mathbf{kG} \\ \mathbf{G}^{\mathrm{T}}\mathbf{k} & \mathbf{G}^{\mathrm{T}}\mathbf{kG} \end{bmatrix}. \tag{41}$$

In this way, the stiffness matrix is derived with respect to the global coordinates which is beneficial from the aspect of the modeling of the system of beams. If necessary, it is straightforward to transform it into the local coordinate system.

The vector of external nodal loads **Q** must be determined similarly as the stiffness matrix, by solving the beam which has the 6$^{\mathrm{th}}$ degree of static indeterminacy. The exceptions are beams for which the basis functions can be derived.

5. Numerical examples

In order to test the present approach, the derived equations are applied for a solution of several benchmark problems, most of them regarding big-curvature beams. The stiffness matrices are calculated firstly, using the BFM procedure. Afterward, unit displacements are enforced on both ends of a beam and exact basis functions are calculated by solving the beam equations where the boundary conditions are obtained utilizing the BFM stiffness matrix. These basis functions are then employed for the derivation of the stiffness matrix by the weak form of equilibrium, [2] and [3], and the result is compared with that from the "exact" BFM approach. For geometries where analytical integration is not possible, the Taylor series approximation of the integrand is applied.

Irrefutably, the BE assumption is violated for big-curvature beams for which the shear strain becomes considerable. As the curviness further increases, the assumption of both beam theories is violated due to the deformation of the cross section. The present contribution explores the accuracy and limits of applicability of the BE beam theory solely.

5.1 Circular beams

This example deals with the simplest 2D curved structures, circular arches. Due to the constant initial curvature, closed-form solutions are feasible and utilized in the presented examples.

5.1.1 Closed-form solution

The stiffness matrix of a big-curvature circular arch is derived in a closed-form using the BFM procedure explained in Section 4 and its elements are given in the Appendix D. Afterward, the basis functions are also derived in a closed-form and the weak form of equilibrium returned exactly the same stiffness matrix. These exact basis functions are somewhat cumbersome due to the analytical integration of section properties and they are omitted here due to the brevity. Additionally, appropriate boundary conditions are applied on these basis functions and the exact rigid body modes are obtained, which again confirms that the presented theory is correct.

In Fig. 4, the basis functions N_1 and N_6 are superposed with the reference geometry of the circular beam *ik* and presented for different values of curviness Kh. Data used for this figure is: x=-$R\cos\xi$, y=$R\sin\xi$, ξ_i=-0.1π, ξ_k=0.7π, b=h=0.2 m, E=1 GPa, R=2 m. It is evident how the increase in curviness influences the contraction of the beam axis due to the increased coupling of the axial and bending actions.

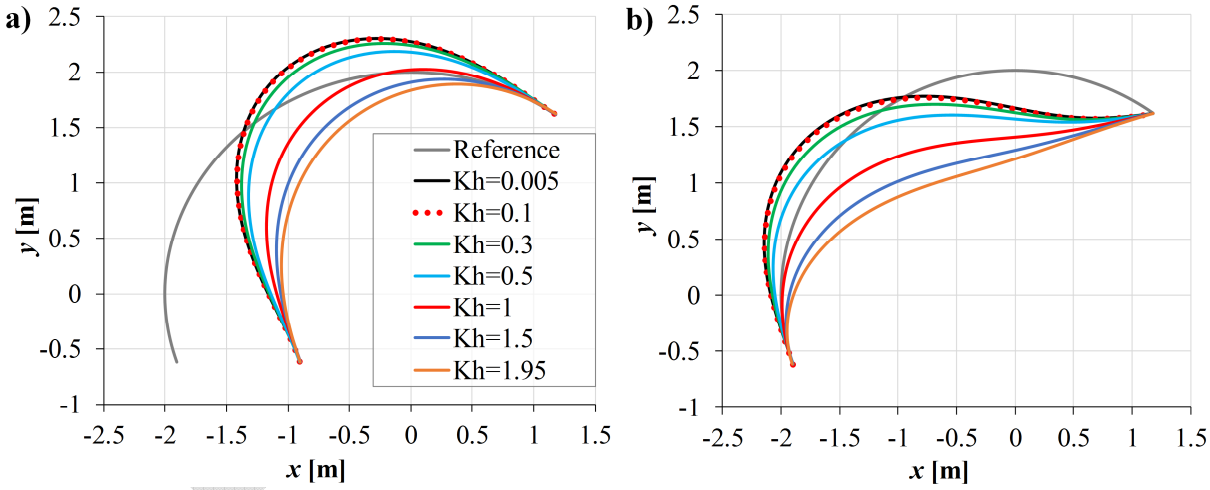

Fig. 4. The circular beam. The basis functions for different values of curviness Kh, superposed with the reference geometry: a) Function N_1 (u_{xi}=1, u_{yi}=φ_{zi}=u_{xk}=u_{yk}=φ_{zk}=0); b) Function N_6 (u_{xi}=u_{yi}=φ_{zi}=u_{xk}=u_{yk}=0, φ_{zk}=1)

5.1.2 Circular ring

The example for which a closed-form solution exists within the scope of the big-curvature theory is considered, [5]. A thick circular ring is loaded with two opposite compressive forces and stresses at the intrados and extrados are observed, Fig. 5a. Due to the symmetry, only a quarter of the beam is analyzed. A complete agreement of stress is obtained by comparison with the solution given in [5]. Numerical values are omitted due to the brevity but the distribution of the stress field is presented in Fig. 5b.

Moreover, an analytical solution for the displacement at the point of force application is found in [18] for the big-curvature theory, in [20] for the small-curvature theory and in [42] for the thin beam model with an inextensible axis. The standard approximation of $1/g_0$ with the 2nd order Taylor polynomial is applied in [18]. These expressions are compared in Table 1 for the beam with a rectangular cross section where $\lambda^2=(Kh)^2/12$. The limit value of the obtained expression as the curviness tends to zero is:

$$\lim_{Kh\to 0}\frac{(Kh)^3\left\{\pi^2\,\mathrm{arcoth}[2/(Kh)]-4Kh\right\}}{96\pi\,\mathrm{arcoth}[2/(Kh)]\left\{Kh\text{-}2\,\mathrm{arcoth}[2/(Kh)]\right\}}=\frac{1}{\pi}-\frac{\pi}{8}, \tag{42}$$

which coincides with the thin beam theory result [42], as well as with the limit value of expressions from [18] and [20]. The relative differences of these displacements are displayed in Fig. 6 for $Kh\in[0.1,1]$. Evidently, differences increase with curviness. Contrary to [42], [18], and [20], no assumptions besides the BE ones are introduced in the present formulation for the linear static analysis

In order to test this result further, a 2D shell model with $Kh=1$ is created using a plane stress/strain section in Abaqus with a fine mesh of 125600 CPS3 elements. In order to make a model which is comparable with big-curvature BE beams, the orthotropic material properties are applied, similar as in [4]. The elasticity modulus along the η direction and the shear modulus are amplified with a factor of $100Kh$, which is empirically determined in [4]. In this way, by setting $b=h=E=P=R=1$, Abaqus returned displacement of 1.0504 while the present approach gave 1.0441, which is an excellent agreement for this high value of curviness.

Table 1. The circular ring. Radial displacement at the point of force application divided by $12P/[Eb(Kh)^3]$. Comparison of expressions obtained by four theories for a rectangular cross section.

Thin beam (inextensible axis) [42]	Thin beam [20]	Thick beam [18]	Present
$\frac{1}{\pi}-\frac{\pi}{8}$	$\frac{1}{\pi}-\frac{\pi}{8}\left(1+\lambda^2\right)$	$\frac{-1}{1+\lambda^2}\left(\frac{\lambda^2}{2}+\frac{1}{2}-\frac{1}{\pi}\right)+\frac{1}{2}-\frac{\pi}{8}$	$\frac{(Kh)^3\left\{\pi^2\,\mathrm{arcoth}[2/(Kh)]-4Kh\right\}}{96\pi\,\mathrm{arcoth}[2/(Kh)]\left\{Kh\text{-}2\,\mathrm{arcoth}[2/(Kh)]\right\}}$

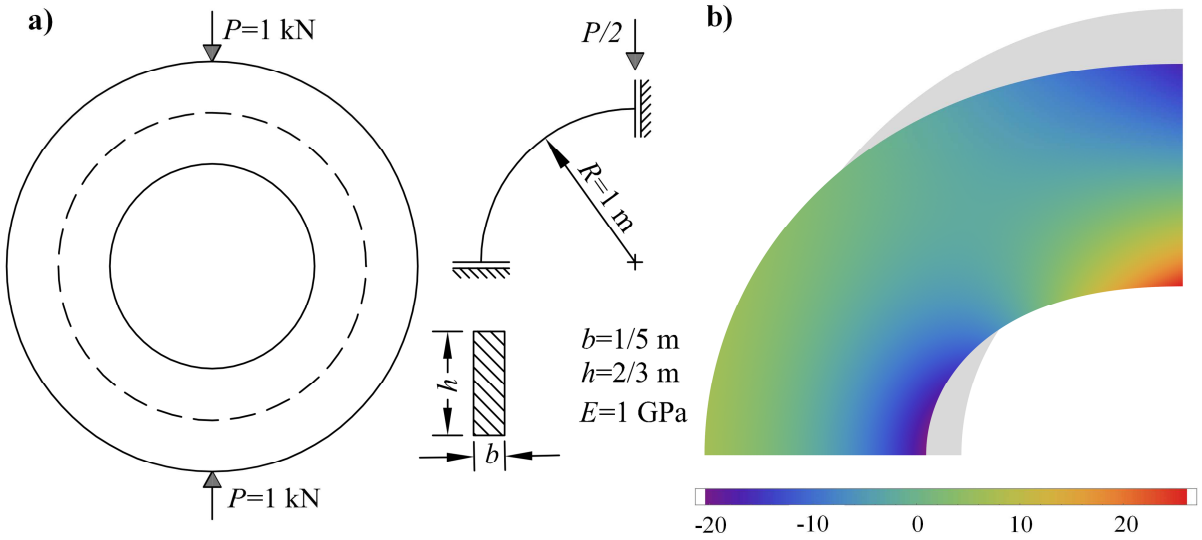

Fig. 5. The circular ring. a) Geometry, material properties, and load disposition; b) Distribution of normal stress [MPa]. Displacements are scaled with a factor of 10000.

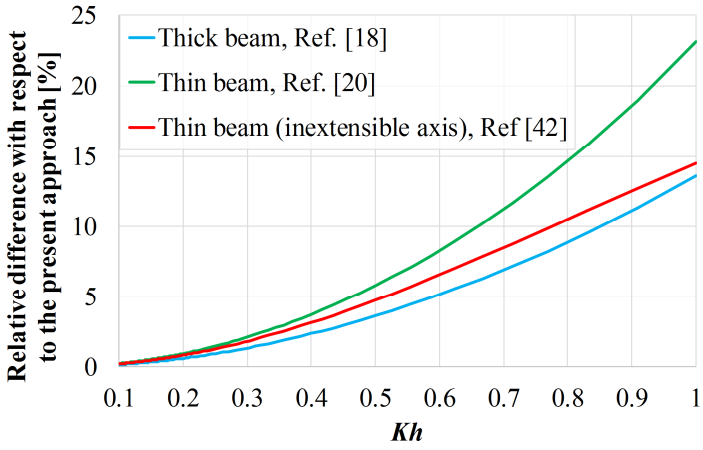

Fig. 6. The circular ring. Comparison of the radial displacement at the point of force application obtained for three different theories vs. curviness *Kh*.

5.1.3 Pre-twisted circular beam

A pre-twisted circular beam, as in Fig. 7, is loaded with a uniformly distributed load p_z=-1 kN/m. The displacement and angle of twist are restrained at the end sections. The most prominent property of this example is the presence of initial twist of the beam cross section. The beam is studied in [41] and [2] using small- and big-curvature IGA models, respectively. Since the numerical analysis in [2] suggested that this example is not affected by the effects of big curvature, the small-curvature model is considered here solely. The vector of external load and end rotations are determined by the flexibility approach and applied as boundary conditions into Eq. (30). The integrals are solved analytically and results for the displacement components and the angle of twist are given in Fig. 8, while distributions of the section forces are displayed in Fig. 9. An excellent agreement of the present analytical results and those from [41] are detected. On the other hand, the discrepancies of numerical IGA results from [2] and the present ones are evident. Since the results in [2] were in the full correspondence with those from Abaqus, this finding asked for a further clarification. Two causes are identified: incorrect parameterization by NURBS and different values of torsion constant. Namely, it is well-known fact that NURBS can exactly describe a circle in a sense that all points lie on the circle, but only the three of these points are at their correct positions, [43]. This introduces an error into the IGA model of circular beams, which is here exaggerated due to the presence of the initial pre-twist. Since the same dataset is used for the definition of the Abaqus model, it returned full correspondence with IGA in [2]. On the other hand, the results in [41] were not affected by this incorrect parameterization since the authors used B-spline interpolation for their IGA model. Furthermore, the observed differences are also caused by the utilization of different coefficients required for the torsion constant of a rectangular cross section with b/h=1/10. The accurate value of this coefficient is used in [2], 0.312, while an approximate one is applied in [41] and here, 0.333. During this research, it is found that the incorrect NURBS parameterization of the circle mostly influences the normal force, while the difference in the torsion constant dominantly affects the angle of twist.

Although it is not the primary objective of this example, it should be noted that the integrals in Eq. (30) could not be solved analytically for the big-curvature beam model.

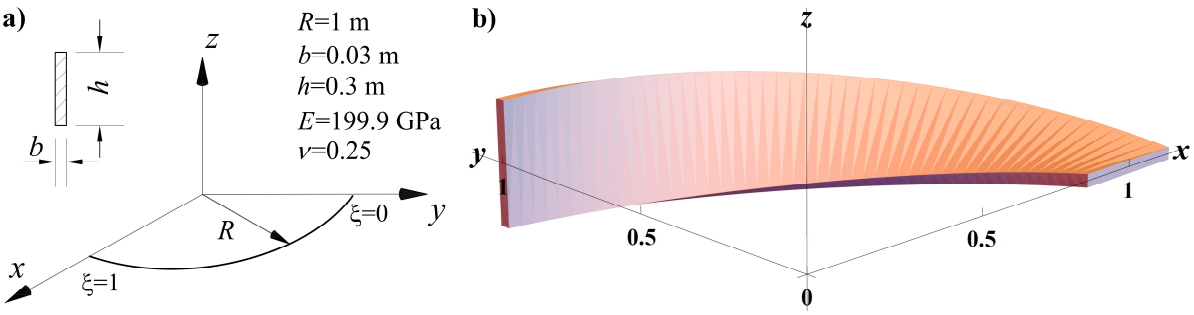

Fig. 7. The pre-twisted beam. a) Geometry and material properties; b) 3D representation.

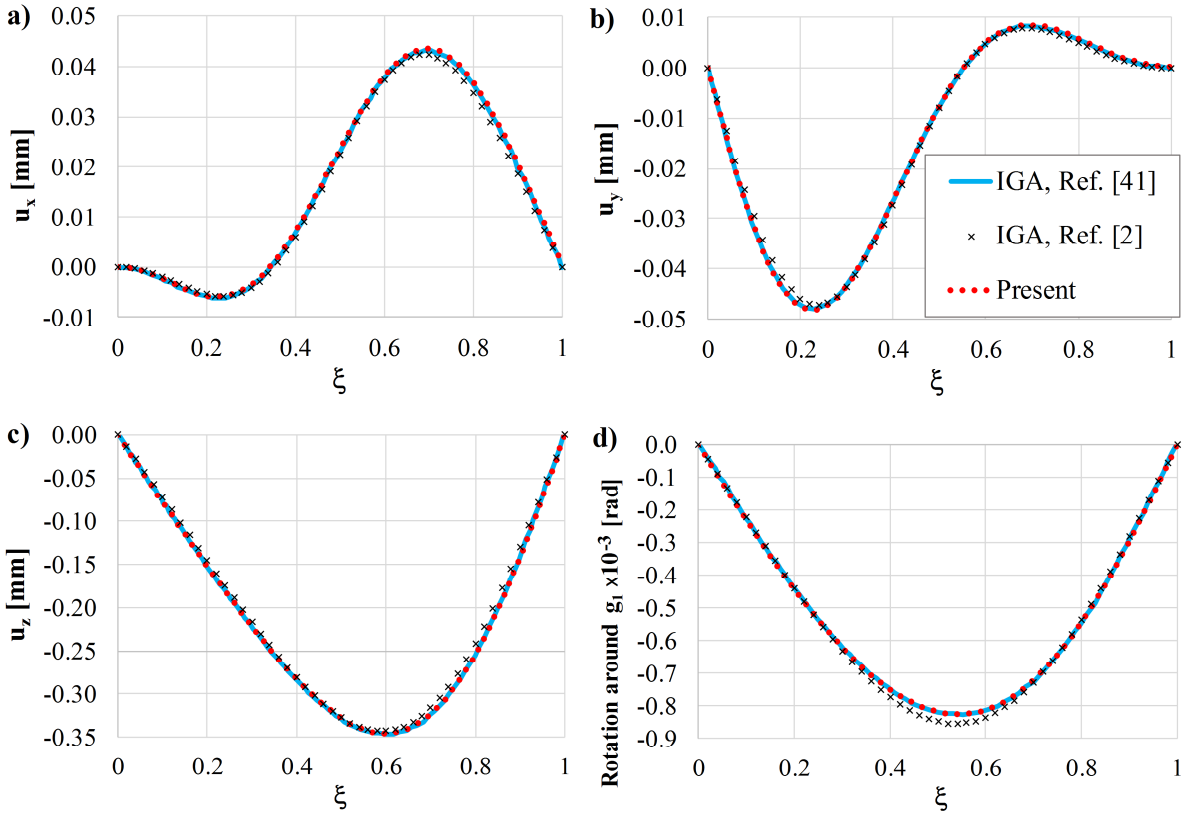

Fig. 8. The pre-twisted beam. Comparison of distributions: a) u_x displacement component; b) u_y displacement component; c) u_z displacement component; d) rotation around $\mathbf{g}_1$ basis.

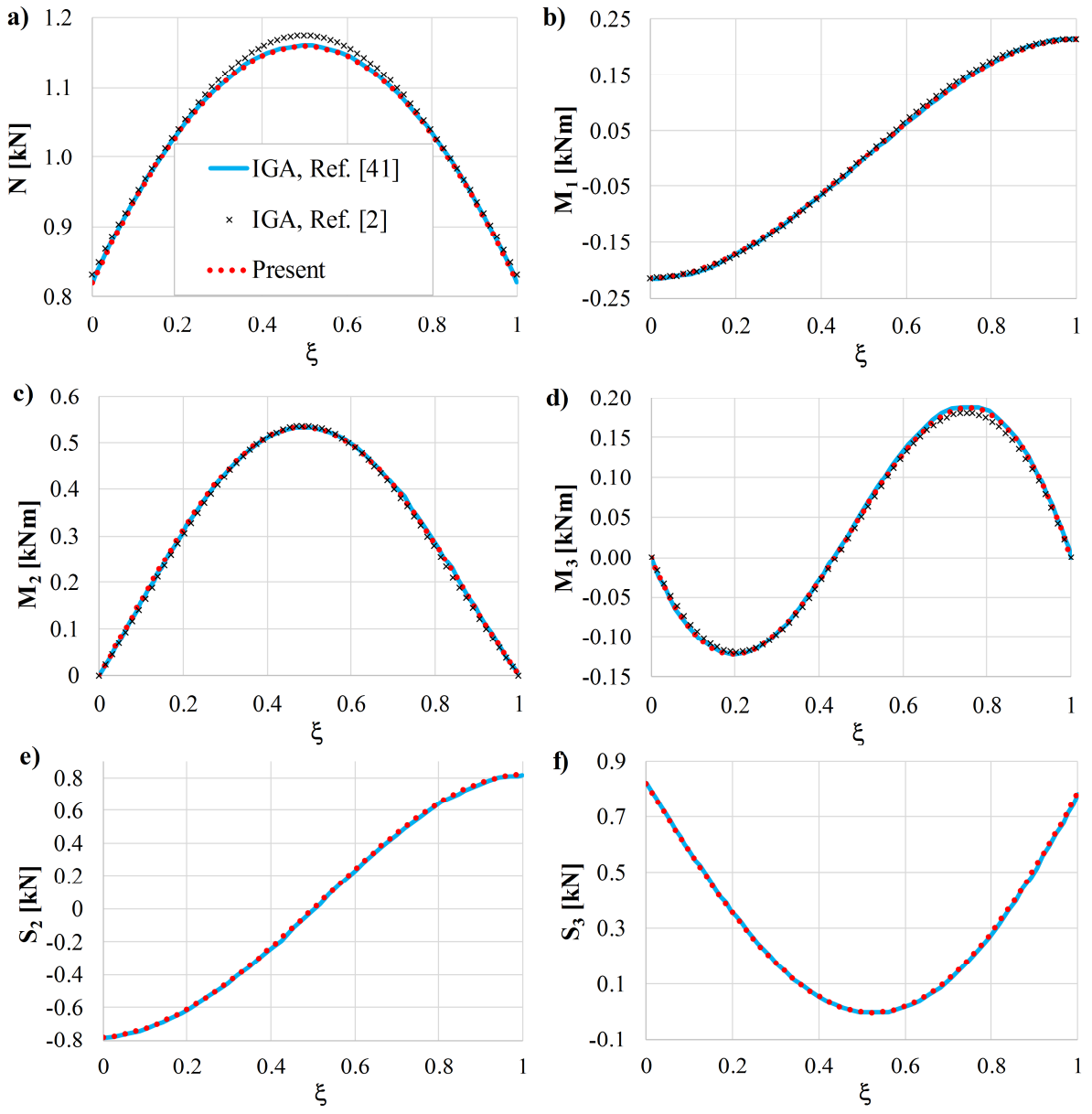

Fig. 9. The pre-twisted beam. Comparison of distributions: a) normal force N; b) torsional moment M_1; c) bending moment M_2; d) bending moment M_3; e) shear force S_2; f) shear force S_3.

5.2 Elliptical ring

An elliptical ring under two equal tensile concentrated forces has been considered, Fig. 10. The properties of double symmetry are utilized and a quarter of the ring is investigated in the simulations. To the best knowledge of the authors, there are no available solutions for the displacements of the points A and B in the literature using the big-curvature BE beam theory. The expression given in [18] does not return an expected result. Moreover, the authors in [5] argue that they had to use the average value of the displacements for the maximum and minimum curvature since it is not possible to integrate appropriate equations using a variable curvature. Note that the curviness KD varies from 3/8 to 8/9 in this example.

The radial displacements u_A=0.649918 mm and u_B=0.623481 mm are obtained using the BFM procedure and they are exactly the same as the ones found with IGA in [3]. Furthermore, the basis functions are derived for this structure and the integrands are approximated with the Taylor series. The convergence of the Taylor series polynomial towards one of the integrand functions is graphically

displayed in Fig. 11a, while the convergence of the appropriate L^2 error norm is given in Fig. 11b. It is interesting that these results are independent of the curviness, although the big-curvature model is utilized. Moreover, the obtained basis functions N_1 and N_6 are given in Fig. 12 for six different values of the curviness $K_{max}D$ and its effect is clearly pronounced, similar as for the circular beam. In the end, the elements of the stiffness matrices obtained with the BFM and weak form are compared with respect to the order of approximation and their relative error is given in Fig. 13 for both the small- and big-curvature models. It is observed that the small-curvature model returns a better accuracy of the stiffness matrix per order of approximation which is caused by the significantly simpler constitutive model.

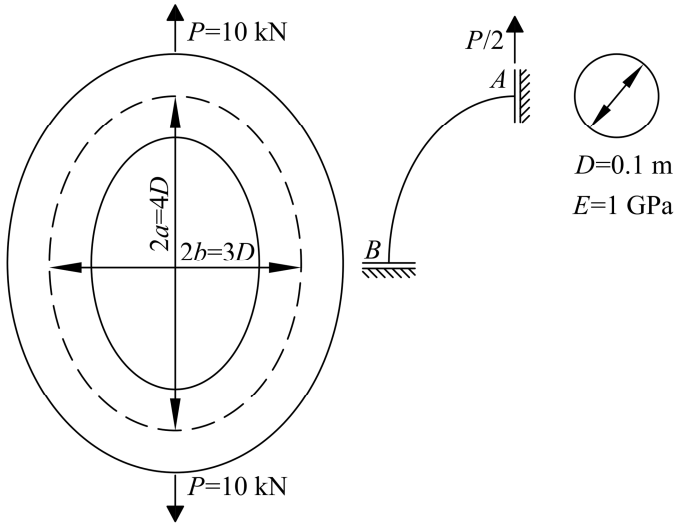

Fig. 10. The elliptical ring. Geometry, material properties, and load disposition.

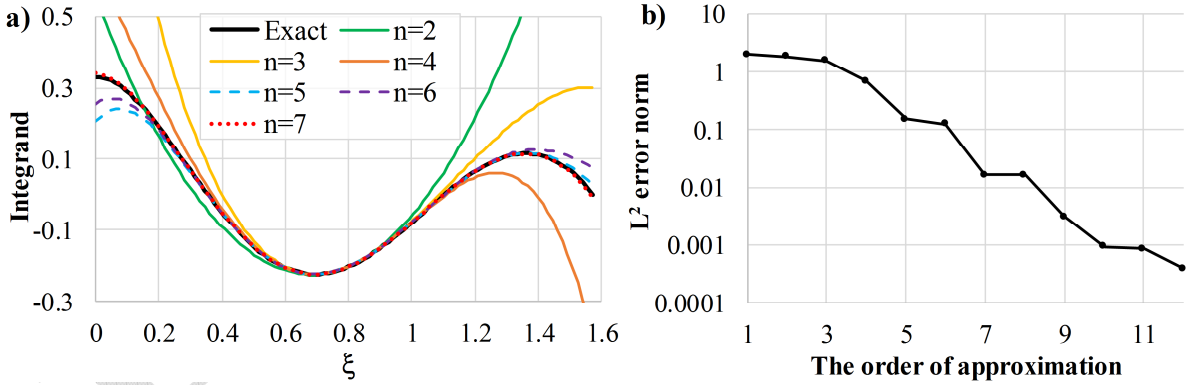

Fig. 11. The elliptical ring. a) Approximation of the integrand function in rotation equation, for the purpose of calculation of basis function N_4 (u_{xi}=u_{yi}=φ_{zi}=u_{yk}=φ_{zk}=0, u_{xk}=1); b) L^2 error norm of this approximation with respect to the order of the Taylor polynomial.

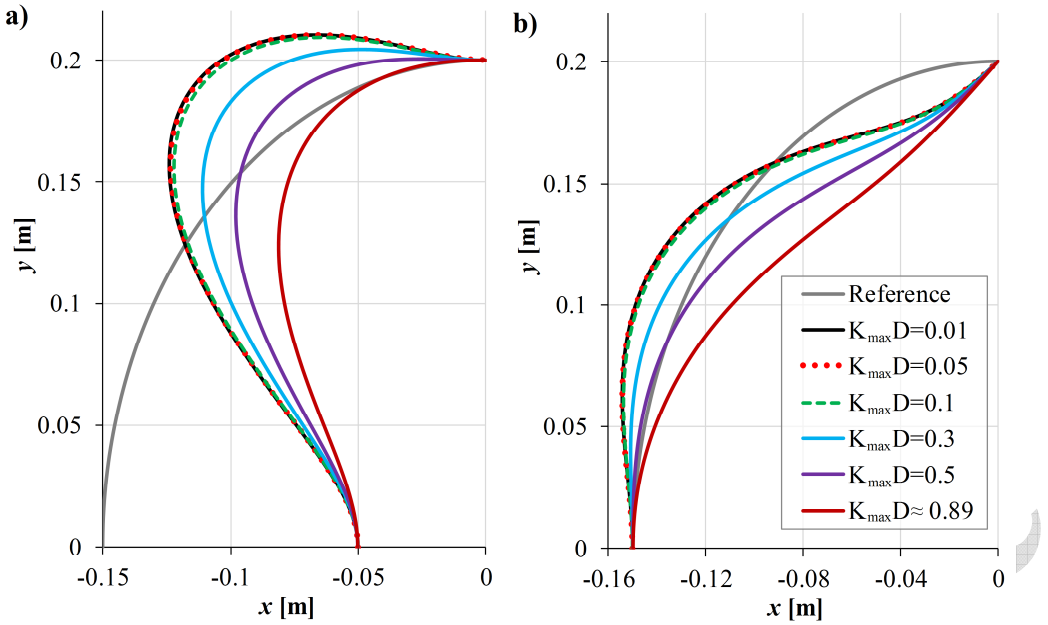

Fig. 12. The elliptical ring. Basis functions for different values of curviness $K_{max}D$, superposed with the reference geometry: a) Function N_1 (u_{xi}=0.1, u_{yi}=φ_{zi}=u_{xk}=u_{yk}=φ_{zk}=0), b) Function N_6 (u_{xi}=u_{yi}=φ_{zi}=u_{xk}=u_{yk}=0, φ_{zk}=1)

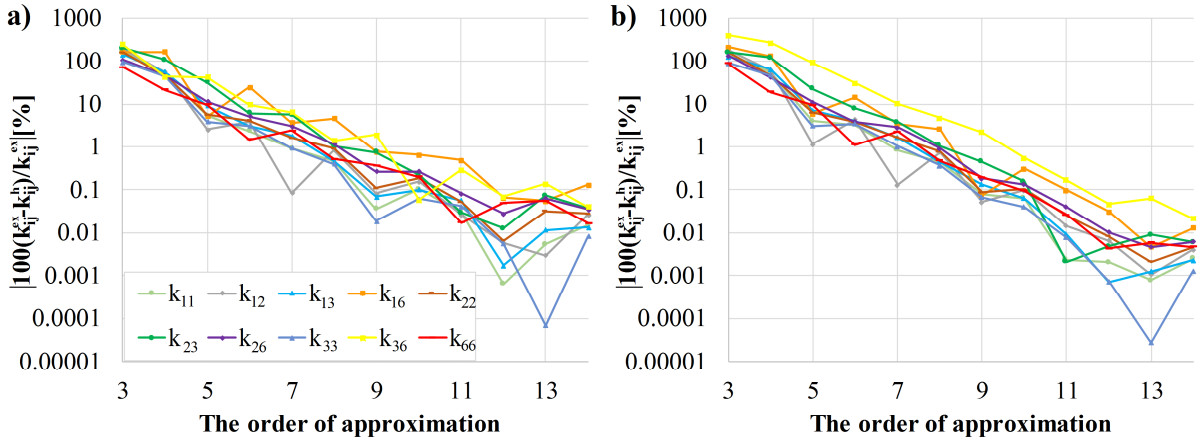

Fig. 13. The elliptical ring. Relative difference of the values of stiffness coefficients calculated by the BFM ("exact") and weak form (approximate) using basis functions obtained by approximation of the integrands with a different polynomial order: a) big-curvature model, b) small-curvature model.

5.3 Circular helix

As the classic example of a spatial beam with constant curvature and torsion, a circular helix with square cross section and without initial twist is analyzed. The axis of the helix is defined with the equations:

$$x(\xi)=a\cos\xi,\quad y(\xi)=a\sin\xi,\quad z(\xi)=b\xi,$$
$$\xi\in[0,3\pi],\quad a=2\,\mathrm{m},\quad b=0.5\,\mathrm{m}. \tag{43}$$

Due to the constant curvature, the basis functions are analytically derived from Eq. (30) and a full agreement of the stiffness matrices using the BFM and weak form is obtained for all values of curviness. The influence of curviness on the basis functions is examined in detail. For u_{xi}=1, the global components of the displacement and the angle of twist are displayed in Fig. 14 where E=30 GPa and ν=0.1. Clearly, the effect of the big curvature is not significantly pronounced in this example, except for the extreme values of the curviness, such as Kh>1. We attribute this fact to the length of the considered beam, which

is not introduced in the adopted parameter of curviness. In order to clearly depict some of the geometries which are studied, the reference geometries of two helices are displayed in Fig. 15 for Kh=0.1 and Kh=0.5. It is evident that the big-curvature helices barely resemble the classic beam geometry.

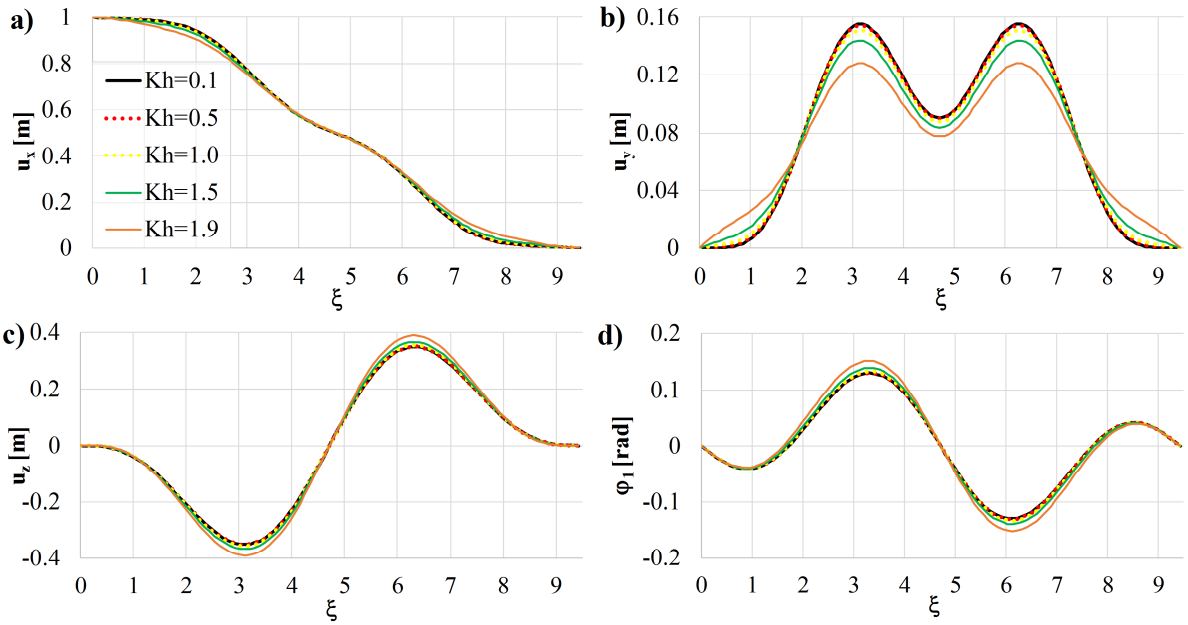

Fig. 14. The circular helix. Components of basis function N_1 (u_{xi}=1, u_{yi}=u_{zi}=φ_{xi}=φ_{yi}=φ_{zi}=u_{xk}=u_{yk}=u_{zk}=φ_{xk}=φ_{yk}=φ_{zk}=0) for different values of curviness Kh: a) displacement component u_x, b) displacement component u_y, c) displacement component u_z, d) rotation component φ_1.

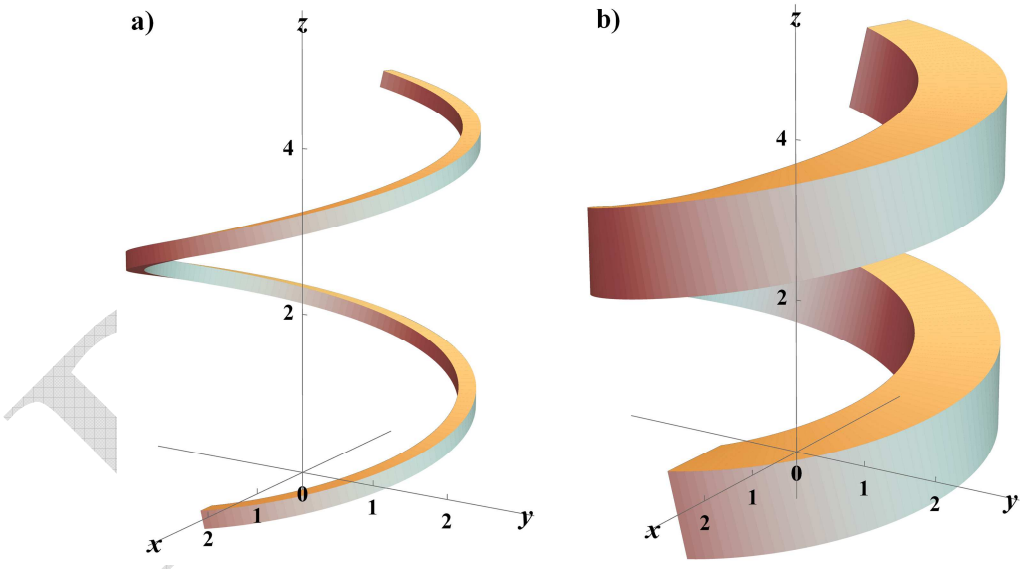

Fig. 15. The circular helix. 3D representation of the reference geometries for two values of curviness: a) Kh=0.1, b) Kh=0.5.

5.4 Cubic NURBS beam

The final example deals with a spatial cantilever loaded with a vertical concentrated force F=1000 kN, Fig. 16. Its axis is parametrized with cubic NURBS where the control points and weights are given in Fig. 16a. The beam is thoroughly analyzed in [2] and the comparison of those results with the analytical ones was one of the driving forces for the present research. Due to the complicated integrands, the analytical solution of appropriate integrals is not viable and a piecewise series approximation of the integrands had to be applied. The approximative polynomials are defined in the

intervals $\xi\in[0,0.5]$ and $\xi\in(0.5,1]$, about their respective middle points. The beam response for b=0.2 m is calculated using the seventh order Taylor polynomial and compared with [2]. The displacement components and the angle of twist are displayed in Fig. 17 where an excellent agreement is evident.

Additionally, the displacement components of the tip of the beam for different values of the curviness $K_{\max}b$ are compared in Table 2. Besides the present big- and small-curvature models, the results are also given for the reduced model developed in [2] with the assumption $g_0=1-\eta K_3+\zeta K_2\approx 1$. The compliance of the results is excellent and the numerical IGA formulation for the linear analysis of big-curvature beams is validated via the comparison with the present approach. It can be noted that the reduced IGA and present small-curvature models return similar results. Still, small differences exist due to the more rigorous constitutive model used in [2].

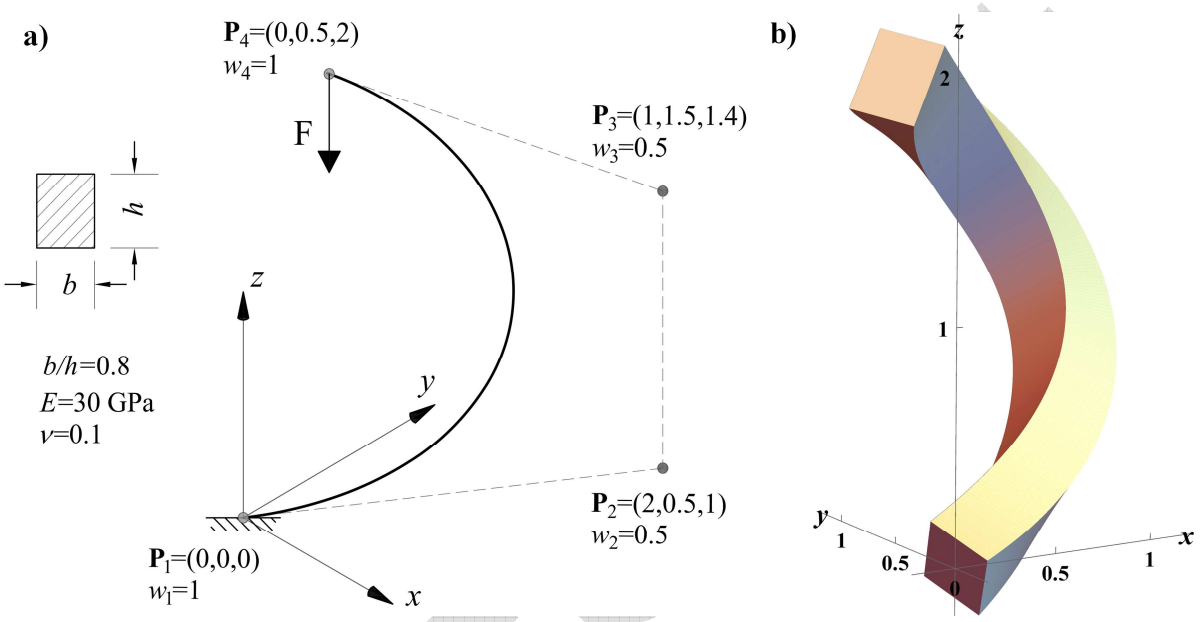

Fig. 16. The cubic beam. a) Geometry, material properties, and load disposition, b) 3D representation for $K_{max}b\approx 0.44$.

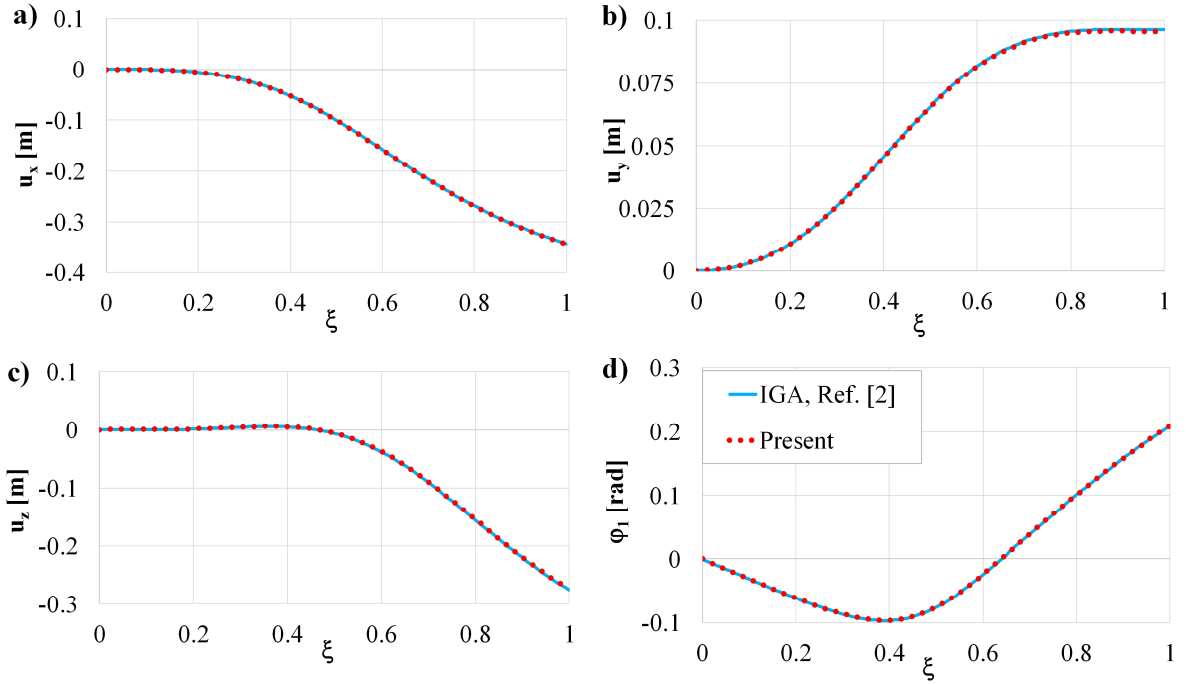

Fig. 17. The cubic beam. Comparison of global displacements components and the angle of twist: a) u_x, b) u_y, c) u_z, d) φ_1.

Table 2. The cubic beam. Comparison of values of the displacement components at the free end for different values of curviness.

	u_x				u_y				u_z			
	IGA [2]		Present		IGA [2]		Present		IGA [2]		Present	
$K_{max}b$	Full	Reduced	Big-curvature	Small-curvature	Full	Reduced	Big-curvature	Small-curvature	Full	Reduced	Big-curvature	Small-curvature
0.074	-88290	-88225	-88289	-88318	24526	24294	24526	24514	-70947	-70908	-70947	-70988
0.148	-5512.6	-5514.0	-5512.6	-5519.8	1534.5	1517.6	1534.5	1531.3	-4429.2	-4434.5	-4429.2	-4439.5
0.296	-343.17	-344.61	-343.17	-344.98	96.292	94.635	96.292	95.492	-275.58	-277.84	-275.58	-278.16
0.444	-67.333	-68.066	-67.333	-68.138	19.149	18.624	19.149	18.793	-54.023	-55.108	-54.023	-55.170
0.592	-21.103	-21.534	-21.103	-21.557	6.1157	5.8618	6.1157	5.9153	-16.909	-17.537	-16.909	-17.556
0.740	-8.5362	-8.8193	-8.5362	-8.8287	2.5349	2.3847	2.5349	2.4067	-6.8280	-7.2356	-6.8280	-7.2436
0.888	-4.0525	-4.2525	-4.0525	-4.2570	1.2402	1.1405	1.2402	1.1510	-3.2342	-3.5204	-3.2342	-3.5243
1.184	-1.2292	-1.3450	-1.2292	-1.3464	0.40670	0.35313	0.40672	0.35648	-0.97470	-1.1389	-0.97468	-1.1401
1.480	-0.47398	-0.55060	-0.47398	-0.55119	0.17423	0.14058	0.17423	0.14195	-0.37198	-0.47963	-0.37198	-0.48013

6. Conclusions

The derived beam equations with respect to the arbitrary parametric coordinate are validated by both correct reduction to the arc-length form and via numerical examples. The curvature change is defined with respect to the convective (arc-length and parametric) and material/spatial coordinates. It is shown that all approaches are in agreement as long as it is clear which quantity and coordinate systems are employed. However, the convective description proves more convenient, which is particularly emphasized in nonlinear analysis.

The exact basis functions are impractical, but comparison with the previous numeric results suggests that high-order NURBS functions with high interelement continuity are an excellent choice for accurate numerical analysis of big-curvature beams. Due to the complicated expressions, the equations

of the big-curvature beam theory are rarely integrable. The Taylor approximation is affirmed as a powerful tool for the analytical assessment of these structures. The problem of more involved parameterization of arbitrary geometries could be addressed by the development of new classes of curves parametrized with the arc-length coordinate, [44].

Further research should be directed toward the analytical approach of free vibration analysis of big-curvature composite and non-uniform beams.

Appendix A

The fact that the Christoffel symbols of the second kind are not tensors is considered. The Christoffel symbols transform as:

$$\overline{\Gamma}^{i}_{jk} = \Gamma^{m}_{nf}\frac{\partial \overline{x}^{i}}{\partial x^{m}}\frac{\partial x^{n}}{\partial \overline{x}^{j}}\frac{\partial x^{f}}{\partial \overline{x}^{k}} + \frac{\partial \overline{x}^{i}}{\partial x^{m}}\frac{\partial^{2} x^{m}}{\partial \overline{x}^{j}\partial \overline{x}^{k}}. \tag{A1}$$

The relation between (s, α, β) and (s, η, ζ) coordinates is, Fig. 1:

$$\begin{aligned} \overline{x}^{2} &= x^{2}\cos\theta + x^{3}\sin\theta, & x^{2} &= \overline{x}^{2}\cos\theta - \overline{x}^{3}\sin\theta, \\ \overline{x}^{3} &= -x^{2}\sin\theta + x^{3}\cos\theta, & x^{3} &= \overline{x}^{2}\sin\theta - \overline{x}^{3}\cos\theta, \end{aligned} \tag{A2}$$

where the coordinates with respect to the (s, η, ζ) system are designated with an overbar. We can easily derive all Christoffel symbols:

$$\begin{aligned} \overline{\Gamma}^{2}_{11} &= \Gamma^{2}_{11}\frac{\partial \overline{x}^{2}}{\partial x^{2}}\left(\frac{\partial x^{1}}{\partial \overline{x}^{1}}\right)^{2} + \Gamma^{1}_{21}\frac{\partial \overline{x}^{2}}{\partial x^{1}}\frac{\partial x^{2}}{\partial \overline{x}^{1}}\frac{\partial x^{1}}{\partial \overline{x}^{1}} + \Gamma^{3}_{21}\frac{\partial \overline{x}^{2}}{\partial x^{3}}\frac{\partial x^{2}}{\partial \overline{x}^{1}}\frac{\partial x^{1}}{\partial \overline{x}^{1}} + \Gamma^{2}_{31}\frac{\partial \overline{x}^{2}}{\partial x^{2}}\frac{\partial x^{3}}{\partial \overline{x}^{1}}\frac{\partial x^{1}}{\partial \overline{x}^{1}} + \\ &+ \frac{\partial \overline{x}^{2}}{\partial x^{1}}\frac{\partial^{2} x^{1}}{\partial \overline{x}^{1}\partial \overline{x}^{1}} + \frac{\partial \overline{x}^{2}}{\partial x^{2}}\frac{\partial^{2} x^{2}}{\partial \overline{x}^{1}\partial \overline{x}^{1}} + \frac{\partial \overline{x}^{2}}{\partial x^{3}}\frac{\partial^{2} x^{3}}{\partial \overline{x}^{1}\partial \overline{x}^{1}} = \Gamma^{2}_{11}\cos\theta = K\cos\theta, \end{aligned} \tag{A3}$$

$$\begin{aligned} \overline{\Gamma}^{1}_{21} &= \Gamma^{2}_{11}\frac{\partial \overline{x}^{1}}{\partial x^{2}}\frac{\partial x^{1}}{\partial \overline{x}^{2}}\frac{\partial x^{1}}{\partial \overline{x}^{1}} + \Gamma^{1}_{21}\frac{\partial \overline{x}^{1}}{\partial x^{1}}\frac{\partial x^{2}}{\partial \overline{x}^{2}}\frac{\partial x^{1}}{\partial \overline{x}^{1}} + \Gamma^{3}_{21}\frac{\partial \overline{x}^{1}}{\partial x^{3}}\frac{\partial x^{2}}{\partial \overline{x}^{2}}\frac{\partial x^{1}}{\partial \overline{x}^{1}} + \Gamma^{2}_{31}\frac{\partial \overline{x}^{1}}{\partial x^{2}}\frac{\partial x^{3}}{\partial \overline{x}^{2}}\frac{\partial x^{1}}{\partial \overline{x}^{1}} + \\ &+ \frac{\partial \overline{x}^{1}}{\partial x^{1}}\frac{\partial^{2} x^{1}}{\partial \overline{x}^{2}\partial \overline{x}^{1}} + \frac{\partial \overline{x}^{1}}{\partial x^{2}}\frac{\partial^{2} x^{2}}{\partial \overline{x}^{2}\partial \overline{x}^{1}} + \frac{\partial \overline{x}^{1}}{\partial x^{3}}\frac{\partial^{2} x^{3}}{\partial \overline{x}^{2}\partial \overline{x}^{1}} = \Gamma^{2}_{21}\cos\theta = -K\cos\theta, \end{aligned} \tag{A4}$$

$$\begin{aligned} \overline{\Gamma}^{3}_{21} &= \Gamma^{2}_{11}\frac{\partial \overline{x}^{3}}{\partial x^{2}}\frac{\partial x^{1}}{\partial \overline{x}^{2}}\frac{\partial x^{1}}{\partial \overline{x}^{1}} + \Gamma^{1}_{21}\frac{\partial \overline{x}^{3}}{\partial x^{1}}\frac{\partial x^{2}}{\partial \overline{x}^{2}}\frac{\partial x^{1}}{\partial \overline{x}^{1}} + \Gamma^{3}_{21}\frac{\partial \overline{x}^{3}}{\partial x^{3}}\frac{\partial x^{2}}{\partial \overline{x}^{2}}\frac{\partial x^{1}}{\partial \overline{x}^{1}} + \Gamma^{2}_{31}\frac{\partial \overline{x}^{3}}{\partial x^{2}}\frac{\partial x^{3}}{\partial \overline{x}^{2}}\frac{\partial x^{1}}{\partial \overline{x}^{1}} + \frac{\partial \overline{x}^{3}}{\partial x^{1}}\frac{\partial^{2} x^{1}}{\partial \overline{x}^{2}\partial \overline{x}^{1}} + \\ &+ \frac{\partial \overline{x}^{3}}{\partial x^{2}}\frac{\partial^{2} x^{2}}{\partial \overline{x}^{2}\partial \overline{x}^{1}} + \frac{\partial \overline{x}^{3}}{\partial x^{3}}\frac{\partial^{2} x^{3}}{\partial \overline{x}^{2}\partial \overline{x}^{1}} = \Gamma^{3}_{21}\cos^{2}\theta + \Gamma^{2}_{31}\left(-\sin^{2}\theta\right) + \left(-\sin\theta\right)\left(-\sin\theta\right)\theta_{,1} + \\ &+ \cos\theta\cos\theta\,\theta_{,1} = \tau\cos^{2}\theta + \tau\sin^{2}\theta + \theta_{,1}\left(\cos^{2}\theta + \sin^{2}\theta\right) = \tau + \theta_{,1}, \end{aligned} \tag{A5}$$

$$\begin{aligned} \overline{\Gamma}^{2}_{31} &= \Gamma^{2}_{11}\frac{\partial \overline{x}^{2}}{\partial x^{2}}\frac{\partial x^{1}}{\partial \overline{x}^{3}}\frac{\partial x^{1}}{\partial \overline{x}^{1}} + \Gamma^{1}_{21}\frac{\partial \overline{x}^{2}}{\partial x^{1}}\frac{\partial x^{2}}{\partial \overline{x}^{3}}\frac{\partial x^{1}}{\partial \overline{x}^{1}} + \Gamma^{3}_{21}\frac{\partial \overline{x}^{2}}{\partial x^{3}}\frac{\partial x^{2}}{\partial \overline{x}^{3}}\frac{\partial x^{1}}{\partial \overline{x}^{1}} + \Gamma^{2}_{31}\frac{\partial \overline{x}^{2}}{\partial x^{2}}\frac{\partial x^{3}}{\partial \overline{x}^{3}}\frac{\partial x^{1}}{\partial \overline{x}^{1}} + \frac{\partial \overline{x}^{2}}{\partial x^{1}}\frac{\partial^{2} x^{1}}{\partial \overline{x}^{3}\partial \overline{x}^{1}} + \\ &+ \frac{\partial \overline{x}^{2}}{\partial x^{2}}\frac{\partial^{2} x^{2}}{\partial \overline{x}^{3}\partial \overline{x}^{1}} + \frac{\partial \overline{x}^{2}}{\partial x^{3}}\frac{\partial^{2} x^{3}}{\partial \overline{x}^{3}\partial \overline{x}^{1}} = \Gamma^{3}_{21}\sin\theta\left(-\sin\theta\right) + \Gamma^{2}_{31}\cos^{2}\theta + \left(\cos\theta\right)\left(-\cos\theta\right)\theta_{,1} + \\ &+ \sin\theta\left(-\sin\theta\right)\theta_{,1} = -\tau\sin^{2}\theta - \tau\cos^{2}\theta - \theta_{,1}\left(\cos^{2}\theta + \sin^{2}\theta\right) = -\tau - \theta_{,1}, \end{aligned} \tag{A6}$$

$$\begin{aligned} \overline{\Gamma}^{3}_{11} &= \Gamma^{2}_{11}\frac{\partial \overline{x}^{3}}{\partial x^{2}}\left(\frac{\partial x^{1}}{\partial \overline{x}^{1}}\right)^{2} + \Gamma^{1}_{21}\frac{\partial \overline{x}^{3}}{\partial x^{1}}\frac{\partial x^{2}}{\partial \overline{x}^{1}}\frac{\partial x^{1}}{\partial \overline{x}^{1}} + \Gamma^{3}_{21}\frac{\partial \overline{x}^{3}}{\partial x^{3}}\frac{\partial x^{2}}{\partial \overline{x}^{1}}\frac{\partial x^{1}}{\partial \overline{x}^{1}} + \Gamma^{2}_{31}\frac{\partial \overline{x}^{3}}{\partial x^{2}}\frac{\partial x^{3}}{\partial \overline{x}^{1}}\frac{\partial x^{1}}{\partial \overline{x}^{1}} + \\ &+ \frac{\partial \overline{x}^{3}}{\partial x^{1}}\frac{\partial^{2} x^{1}}{\partial \overline{x}^{1}\partial \overline{x}^{1}} + \frac{\partial \overline{x}^{3}}{\partial x^{2}}\frac{\partial^{2} x^{2}}{\partial \overline{x}^{1}\partial \overline{x}^{1}} + \frac{\partial \overline{x}^{3}}{\partial x^{3}}\frac{\partial^{2} x^{3}}{\partial \overline{x}^{1}\partial \overline{x}^{1}} = \Gamma^{2}_{11}\left(-\sin\theta\right) = -K\sin\theta. \end{aligned} \tag{A7}$$

In other words, if we observe these two matrices:

$$K_{ij}=\begin{bmatrix}0 & K & 0\\ -K & 0 & \tau\\ 0 & -\tau & 0\end{bmatrix},\ \bar{K}_{ij}=\begin{bmatrix}0 & K\cos\theta & -K\sin\theta\\ -K\cos\theta & 0 & \tau+\theta_{,1}\\ K\sin\theta & -\left(\tau+\theta_{,1}\right) & 0\end{bmatrix}, \tag{A8}$$

the following is valid:

$$\begin{aligned}&\bar{K}_{12}=K_{ij}\frac{\partial x^i}{\partial\bar{x}^1}\frac{\partial x^j}{\partial\bar{x}^2},\ \ \bar{K}_{13}=K_{ij}\frac{\partial x^i}{\partial\bar{x}^1}\frac{\partial x^j}{\partial\bar{x}^3},\ \ \bar{K}_{21}=K_{ij}\frac{\partial x^i}{\partial\bar{x}^2}\frac{\partial x^j}{\partial\bar{x}^1},\ \ \bar{K}_{31}=K_{ij}\frac{\partial x^i}{\partial\bar{x}^3}\frac{\partial x^j}{\partial\bar{x}^1}\\ &\bar{K}_{23}\neq K_{ij}\frac{\partial x^i}{\partial\bar{x}^2}\frac{\partial x^j}{\partial\bar{x}^3},\ \ \bar{K}_{32}\neq K_{ij}\frac{\partial x^i}{\partial\bar{x}^3}\frac{\partial x^j}{\partial\bar{x}^2}.\end{aligned} \tag{A9}$$

It is clear that the curvature parts of the Christoffel symbols transform as tensor components but the torsion parts do not. For surfaces, the Christoffel symbols with index 3 in the superscript always transform as tensors since the basis vector $\mathbf{g}_3$ (normal to the surface) is constant:

$$\begin{aligned}&\bar{\Gamma}^3_{\alpha\beta}=\Gamma^i_{jk}\frac{\partial\bar{x}^3}{\partial x^i}\frac{\partial x^j}{\partial\bar{x}^\alpha}\frac{\partial x^k}{\partial\bar{x}^\beta}+\frac{\partial\bar{x}^3}{\partial x^i}\frac{\partial^2 x^i}{\partial\bar{x}^\alpha\partial\bar{x}^\beta}=\Gamma^3_{\mu\nu}\frac{\partial x^\mu}{\partial\bar{x}^\alpha}\frac{\partial x^\nu}{\partial\bar{x}^\beta}+\frac{\partial\bar{x}^3}{\partial x^3}\frac{\partial^2 x^3}{\partial\bar{x}^\alpha\partial\bar{x}^\beta}=\Gamma^3_{\mu\nu}\frac{\partial x^\mu}{\partial\bar{x}^\alpha}\frac{\partial x^\nu}{\partial\bar{x}^\beta},\\ &\bar{b}_{\alpha\beta}=b_{\mu\nu}\frac{\partial x^\mu}{\partial\bar{x}^\alpha}\frac{\partial x^\nu}{\partial\bar{x}^\beta},\ \ \bar{x}^3=x^3=const.\end{aligned} \tag{A10}$$

However, the other Christoffel symbols of the second kind on surface are not tensors.

Appendix B

It is not trivial to find the proper change of the curvature with respect to the arc-length coordinate. The main problem is that the curvatures in the deformed and reference configurations are defined with respect to the different coordinate systems since the arc-length coordinate changes with the deformation of the beam axis. We have two options here. The first one is to express the curvature of the deformed configuration with respect to the reference configuration, and this is discussed in the Appendix C. A more elegant approach is to assign the convective property to the arc-length coordinate. For this case, the tangential base vector of the deformed axis is no longer a unit vector. Without the loss of generality, we will look at the case of θ=0 for which K_3=K and K_2=0. The position vector of the beam axis in the deformed configuration and the displacement vector are:

$$\mathbf{r}^*=\mathbf{r}+\mathbf{u},\quad \mathbf{u}=u_k\mathbf{g}^k=\bar{u}_k\mathbf{t}^k,\quad \mathbf{t}^k=[\mathbf{t},\mathbf{n},\mathbf{b}]. \tag{B1}$$

The components of displacement and rotation with respect to the FS coordinates will be designated with an overbar in the appendices. The relations between partial derivatives of the displacement vector with respect to the parametric and arc-length coordinates are:

$$\begin{aligned}&\mathbf{u}_{,\xi}=\frac{\mathrm{d}\mathbf{u}}{\mathrm{d}\xi}=\frac{\mathrm{d}\mathbf{u}}{\mathrm{d}s}\frac{\mathrm{d}s}{\mathrm{d}\xi}=\sqrt{g}\mathbf{u}_{,s},\\ &\mathbf{u}_{,\xi\xi}=\sqrt{g}\left(\sqrt{g}\mathbf{u}_{,s}\right)_{,s}=\sqrt{g}\left(\sqrt{g}\mathbf{u}_{,ss}+\frac{g_{,\xi}}{2g}\mathbf{u}_{,s}\right)=\sqrt{g}\left(\sqrt{g}\mathbf{u}_{,ss}+\Gamma^1_{11}\mathbf{u}_{,s}\right)=g\mathbf{u}_{,ss}+\sqrt{g}\Gamma^1_{11}\mathbf{u}_{,s},\end{aligned} \tag{B2}$$

while the relations between covariant derivatives of the components of rotation are:

$$\varphi_{1|\xi}=g\bar{\varphi}_{1|s},\quad \varphi_{2|\xi}=\sqrt{g}\bar{\varphi}_{2|s},\quad \varphi_{3|\xi}=\sqrt{g}\bar{\varphi}_{3|s}. \tag{B3}$$

Designations $()_{,\xi}$, $()_{|\xi}$, and $()_{,s}$,$()_{|s}$ are utilized in order to distinguish derivatives with respect to the parametric and arc-length coordinates, respectively.

The base vectors of the deformed configuration are:

$$\begin{aligned}\mathbf{g}_1^* &= \frac{\mathrm{d}\mathbf{r}^*}{\mathrm{d}s} = (1+\bar{u}_{1|s})\mathbf{t} + \bar{u}_{2|s}\mathbf{n} + \bar{u}_{3|s}\mathbf{b},\\ \mathbf{g}_2^* &= \mathbf{n} + \boldsymbol{\varphi}\times\mathbf{n} = \mathbf{n} + \bar{\varphi}_1\mathbf{b} - \bar{\varphi}_3\mathbf{t},\\ \mathbf{g}_3^* &= \mathbf{b} + \boldsymbol{\varphi}\times\mathbf{b} = \mathbf{b} - \bar{\varphi}_1\mathbf{n} + \bar{\varphi}_2\mathbf{t},\end{aligned} \tag{B4}$$

while the first derivative of $\mathbf{g}_1^*$ basis is:

$$\begin{aligned}\mathbf{g}_{1,s}^* &= \frac{\mathrm{d}\mathbf{g}_1^*}{\mathrm{d}s} = (\bar{u}_{1|s})_{,s}\mathbf{t} + (\bar{u}_{2|s})_{,s}\mathbf{n} + (\bar{u}_{3|1})_{,s}\mathbf{b} + (1+\bar{u}_{1|s})K\mathbf{n} + \bar{u}_{2|s}(-K\mathbf{t}+\tau\mathbf{b}) - \bar{u}_{3|s}\tau\mathbf{n}\\ &= \left[(\bar{u}_{1|s})_{,s} - K\bar{u}_{2|s}\right]\mathbf{t} + \left[(\bar{u}_{2|s})_{,s} + K(1+\bar{u}_{1|s}) - \tau\bar{u}_{3|s}\right]\mathbf{n} + \left[(\bar{u}_{3|s})_{,s} + \tau\bar{u}_{2|s}\right]\mathbf{b}.\end{aligned} \tag{B5}$$

Using Eq. (B4) and (B5), the curvature K_3^* is:

$$K_3^* = \mathbf{g}_{1,s}^*\cdot\mathbf{g}_2^* = (\bar{u}_{2|s})_{,s} - \tau\bar{u}_{3|s} + K(1+\bar{u}_{1|s}) + \bar{\varphi}_1\left[(\bar{u}_{3|s})_{,s} + \tau\bar{u}_{2|s}\right] - \bar{\varphi}_3\left[(\bar{u}_{1|s})_{,s} - K\bar{u}_{2|s}\right], \tag{B6}$$

which can be linearized with respect to the reference configuration:

$$K_3^* \approx K + (\bar{u}_{2|s})_{,s} - \tau\bar{u}_{3|s} + K\bar{u}_{1|s}. \tag{B7}$$

The curvatures in both configurations are now expressed with respect to the same convective arc-length coordinate s and the curvature change is:

$$\chi_3(s) = K_3^*(s) - K(s) = (\bar{u}_{2|s})_{,s} - \tau\bar{u}_{3|s} + K\bar{u}_{1|s} = \bar{\varphi}_{3,s} + \tau\bar{\varphi}_2 + K\varepsilon_{(11)} = \bar{\varphi}_{3|s} + K\varepsilon_{(11)}, \tag{B8}$$

where the parentheses in the index of the axial strain $\varepsilon_{(11)}$ designate the physical component. Similarly, the other component of the curvature in the deformed configuration is:

$$\begin{aligned}-K_2^* &= \mathbf{g}_{1,s}^*\cdot\mathbf{g}_3^* = (\bar{u}_{3|s})_{,s} + \tau\bar{u}_{2|s} - \bar{\varphi}_1\left[(\bar{u}_{2|s})_{,s} + K(1+\bar{u}_{1|s}) - \tau\bar{u}_{3|s}\right] + \bar{\varphi}_2\left[(\bar{u}_{1|s})_{,s} - K\bar{u}_{2|s}\right] \approx\\ &\approx (\bar{u}_{3|s})_{,s} + \tau\bar{u}_{2|s} - K\bar{\varphi}_1 = -\bar{\varphi}_{2,s} - K\bar{\varphi}_1 + \tau\bar{\varphi}_3 = -(\bar{\varphi}_{2,s} + K\bar{\varphi}_1 - \tau\bar{\varphi}_3) = -\bar{\varphi}_{2|s}.\end{aligned} \tag{B9}$$

For the calculation of the torsion in the deformed configuration, the derivative of the base vector $\mathbf{g}_3^*$ is required:

$$\begin{aligned}\mathbf{g}_{3,s}^* &= \mathbf{b}_{,s} - \bar{\varphi}_{1,s}\mathbf{n} - \bar{\varphi}_1\mathbf{n}_{,s} + \bar{\varphi}_{2,s}\mathbf{t} + \bar{\varphi}_2\mathbf{t}_{,s} = -\tau\mathbf{n} - \bar{\varphi}_{1,s}\mathbf{n} - \bar{\varphi}_1(-K\mathbf{t}+\tau\mathbf{b}) + \bar{\varphi}_{2,s}\mathbf{t} + \bar{\varphi}_2 K\mathbf{n}\\ &= -(\tau + \bar{\varphi}_{1,s} - K\bar{\varphi}_2)\mathbf{n} + (K\bar{\varphi}_1 + \bar{\varphi}_{2,s})\mathbf{t} - \tau\bar{\varphi}_1\mathbf{b},\end{aligned} \tag{B10}$$

which gives:

$$\begin{aligned}-K_1^* &= \mathbf{g}_{3,s}^*\cdot\mathbf{g}_2^* = -(\tau + \bar{\varphi}_{1,s} - K\bar{\varphi}_2) - \tau\bar{\varphi}_1 - (K\bar{\varphi}_1 + \bar{\varphi}_{2,s})\bar{\varphi}_3\\ &\approx -(\tau + \bar{\varphi}_{1,s} - K\bar{\varphi}_2) = -K_1 - (\bar{\varphi}_{1,s} - K\bar{\varphi}_2) = -K_1 - \bar{\varphi}_{1|s}.\end{aligned} \tag{B11}$$

Finally, the derived expressions (B8), (B9), and (B11) can be easily generalized for the case of $\theta\neq 0$:

$$\bar{\varphi}_{1|s} = \chi_1, \quad \bar{\varphi}_{2|s} = \chi_2 - K_2\varepsilon_{(11)}, \quad \bar{\varphi}_{3|s} = \chi_3 - K_3\varepsilon_{(11)}. \tag{B12}$$

Let us now rearrange and compare equations (23) and (B12):

$$\begin{aligned}&\kappa_1 = \frac{1}{\sqrt{g}}\varphi_{1|\xi}, \qquad \kappa_2 = \sqrt{g}\varphi_{2|\xi} + K_2\varepsilon_{11}, \quad \kappa_3 = \sqrt{g}\varphi_{3|\xi} + K_3\varepsilon_{11},\\ &\chi_1 = \bar{\varphi}_{1|s}, \qquad \chi_2 = \bar{\varphi}_{2|s} + K_2\varepsilon_{(11)}, \qquad \chi_3 = \bar{\varphi}_{3|s} + K_3\varepsilon_{(11)}.\end{aligned} \tag{B13}$$

In this way, simple relations between the curvature changes with respect to the parametric and arc-length convective coordinates are revealed:

$$\begin{aligned}
\kappa_1 &= \frac{1}{\sqrt{g}}\varphi_{1|\xi} = \sqrt{g}\chi_1, \\
\kappa_2 &= \sqrt{g}\varphi_{2|\xi} + K_2\varepsilon_{11} = g\left(\chi_2 - K_2\varepsilon_{(11)}\right) + K_2\varepsilon_{11} = g\chi_2, \\
\kappa_3 &= \sqrt{g}\varphi_{3|\xi} + K_3\varepsilon_{11} = g\left(\chi_3 - K_3\varepsilon_{(11)}\right) + K_3\varepsilon_{11} = g\chi_3.
\end{aligned} \tag{B14}$$

For g=1, these quantities are equal, which was to be demonstrated.

Furthermore, let us find the curvature changes with respect to the FS frame as functions of displacement of the beam axis and the angle of twist of cross section. If we note that:

$$\hat{\varphi}^1_{,\xi} = \sqrt{g}\overline{\varphi}^1_{,s}, \tag{B15}$$

Eq. (20) becomes:

$$\begin{aligned}
\kappa_1 &= \sqrt{g}\left(K_2\overline{u}_{2|s} + K_3\overline{u}_{3|s} + \overline{\varphi}_{1,s}\right), \\
\kappa_2 &= -\mathbf{g}_3\cdot\left(g\mathbf{u}_{,ss} + \sqrt{g}\Gamma^1_{11}\mathbf{u}_{,s} - \Gamma^1_{11}\sqrt{g}\mathbf{u}_{,s}\right) + gK_3\hat{\varphi}^1 = g\left(-\mathbf{g}_3\cdot\mathbf{u}_{,ss} + K_3\overline{\varphi}_1\right), \\
\kappa_3 &= \mathbf{g}_2\cdot\left(g\mathbf{u}_{,ss} + \sqrt{g}\Gamma^1_{11}\mathbf{u}_{,s} - \Gamma^1_{11}\sqrt{g}\mathbf{u}_{,s}\right) - gK_2\hat{\varphi}^1 = g\left(\mathbf{g}_2\cdot\mathbf{u}_{,ss} - K_2\overline{\varphi}_1\right).
\end{aligned} \tag{B16}$$

Required relations now follow from Eq. (B16) and (B14):

$$\begin{aligned}
\chi_1 &= K_2\overline{u}_{2|s} + K_3\overline{u}_{3|s} + \overline{\varphi}_{1,s}, \\
\chi_2 &= -\mathbf{g}_3\cdot\mathbf{u}_{,ss} + K_3\overline{\varphi}_1, \\
\chi_3 &= \mathbf{g}_2\cdot\mathbf{u}_{,ss} - K_2\overline{\varphi}_1.
\end{aligned} \tag{B17}$$

Appendix C

If we do not impose the convective property to the FS frame of reference, the curvature change is a difference between the curvatures of spatial and material configurations, χ_s=$K^*(s^*)$-$K(s)$. The problem arises because the coordinate itself is changed due to the deformation. Therefore, the curvature in the deformed configuration (spatial coordinates) $K^*(s^*)$ will be expressed as a function of reference configuration (material coordinates) $K^*(s)$.

Firstly, the tangent of the deformed axis will be represented as:

$$\mathbf{t}^* = \frac{\mathrm{d}\mathbf{r}^*}{\mathrm{d}s^*} = \frac{\mathrm{d}\mathbf{r}^*}{\mathrm{d}s}\frac{\mathrm{d}s}{\mathrm{d}s^*} = \frac{1}{\sqrt{\hat{g}^*}}\left[\left(1+\overline{u}_{1|s}\right)\mathbf{t} + \overline{u}_{2|s}\mathbf{n} + \overline{u}_{3|s}\mathbf{b}\right], \tag{C1}$$

where the relation between spatial and material arc-length coordinates of both configurations is:

$$\mathrm{d}s^* = \sqrt{\hat{g}^*}\mathrm{d}s, \quad \hat{g}^* = \left(1+\overline{u}_{1|s}\right)^2 + \left(\overline{u}_{2|s}\right)^2 + \left(\overline{u}_{3|s}\right)^2. \tag{C2}$$

It follows that the change of the tangent can be calculated as:

$$\begin{aligned}
\frac{\mathrm{d}\mathbf{t}^*}{\mathrm{d}s^*} = K^*\mathbf{n}^* = \frac{1}{\hat{g}^*}\left\{\left[\left(\overline{u}_{1|s}\right)_{,s} - K\overline{u}_{2|s}\right]\mathbf{t} + \left[\left(\overline{u}_{2|s}\right)_{,s} + K\left(1+\overline{u}_{1|s}\right) - \tau\overline{u}_{3|s}\right]\mathbf{n} + \left[\left(\overline{u}_{3|s}\right)_{,s} + \tau\overline{u}_{2|s}\right]\mathbf{b}\right\} - \\
- \frac{1}{\hat{g}^{*2}}\left[\left(1+\overline{u}_{1|s}\right)\mathbf{t} + \overline{u}_{2|s}\mathbf{n} + \overline{u}_{3|s}\mathbf{b}\right]\left[\left(1+\overline{u}_{1|s}\right)\left(\overline{u}_{1|s}\right)_{,s} + \overline{u}_{2|s}\left(\overline{u}_{2|s}\right)_{,s} + \overline{u}_{3|s}\left(\overline{u}_{3|s}\right)_{,s}\right].
\end{aligned} \tag{C3}$$

This expression is exact but too cumbersome, and it will be linearized. For that, let us refer to the linearized expression for the normal in the deformed configuration, derived in the Appendix of [2]. For (s, α, β) coordinates it reduces to:

$$\mathbf{n}^* \approx \mathbf{n} + \frac{1}{K}\left[\mathbf{b}\cdot\mathbf{u}_{,ss}\right]\mathbf{b} - \left(\mathbf{n}\cdot\mathbf{u}_{,s}\right)\mathbf{t} = -\overline{u}_{2|s}\mathbf{t} + \mathbf{n} + \frac{1}{K}\left[\left(\overline{u}_{3|s}\right)_{,s} + \tau\overline{u}_{2|s}\right]\mathbf{b}. \tag{C4}$$

Furthermore, linearization of the following quantities is required:

$$\begin{aligned} \frac{1}{\hat{g}^*} &\approx 1 - \frac{1}{\hat{g}^{*2}}2\left(1+\overline{u}_{1|s}\right)\Big|_{u_i=0}\ \overline{u}_{1|s} = 1 - 2\varepsilon_{(11)}, \\ \frac{1}{\hat{g}^{*2}} &\approx 1 - \frac{2}{\hat{g}^{*3}}2\left(1+\overline{u}_{1|s}\right)\Big|_{u_i=0}\ \overline{u}_{1|s} = 1 - 4\varepsilon_{(11)}. \end{aligned} \tag{C5}$$

Now, inserting Eq. (C4) and (C5) into (C3) gives the linearized change of tangent:

$$\begin{aligned} \frac{d\mathbf{t}^*}{ds^*} = \left(1-2\varepsilon_{(11)}\right)\left\{\left[\left(\overline{u}_{1|s}\right)_{,s} - K\overline{u}_{2|s}\right]\mathbf{t} + \left[\left(\overline{u}_{2|s}\right)_{,s} + K\left(1+\overline{u}_{1|s}\right) - \tau\overline{u}_{3|s}\right]\mathbf{n} + \left[\left(\overline{u}_{3|s}\right)_{,s} + \tau\overline{u}_{2|s}\right]\mathbf{b}\right\} - \\ -\left(1-4\varepsilon_{(11)}\right)\left[\left(1+\overline{u}_{1|s}\right)\mathbf{t} + \overline{u}_{2|s}\mathbf{n} + \overline{u}_{3|s}\mathbf{b}\right]\left[\left(1+\overline{u}_{1|s}\right)\left(\overline{u}_{1|s}\right)_{,s} + \overline{u}_{2|s}\left(\overline{u}_{2|s}\right)_{,s} + \overline{u}_{3|s}\left(\overline{u}_{3|s}\right)_{,s}\right], \end{aligned} \tag{C6}$$

which returns the curvature of the deformed axis as a function of the material coordinate s:

$$\begin{aligned} K^*(s) &= \frac{d\mathbf{t}^*}{ds^*}\cdot\mathbf{n}^* = \left(1-2\varepsilon_{(11)}\right)\left[\left(\overline{u}_{2|s}\right)_{,s} + K\left(1+\overline{u}_{1|s}\right) - \tau\overline{u}_{3|s}\right] \approx \left(\overline{u}_{2|s}\right)_{,s} + K\left(1+\varepsilon_{(11)}\right) - \tau\overline{u}_{3|s} - 2K\varepsilon_{(11)} \\ &= \overline{\varphi}_{3,s} + \tau\overline{\varphi}_2 + K + K\varepsilon_{(11)} - 2K\varepsilon_{(11)} = K + \overline{\varphi}_{3|s} - K\varepsilon_{(11)}. \end{aligned} \tag{C7}$$

The higher order terms of strains and displacement gradients are neglected since we are dealing with the linear analysis. Using Eq. (B12) with $\chi=\chi_3$ and $K=K_3$, the curvature change is:

$$\chi_s(s) = K^*(s^*) - K(s) = \overline{\varphi}_{3|s} - K\varepsilon_{(11)} = \chi - 2K\varepsilon_{(11)}. \tag{C8}$$

The two measures of the curvature change, χ_s and χ, differ for a factor $2K\varepsilon_{(11)}$. The derived expression (C8) contains the Kirchhoff-Clebsch parameter of the flexural strain, [1], [9], that is actually the covariant derivative of rotation:

$$\overline{\varphi}_{3|s} = \chi_s + K\varepsilon_{(11)}. \tag{C9}$$

This parameter is unsuitably compared with the curvature change with respect to the convective coordinate, κ, in [3]. The correct reasoning follows from the fact that the metric coefficient $g_{11}{}^*=g^*$ in the deformed configuration is:

$$\varepsilon_{11} = \frac{1}{2}(g_{11}^* - g_{11}) \Rightarrow g_{11}^* = g_{11} + 2\varepsilon_{11}, \tag{C10}$$

which gives the curvature change with respect to the convective parametric coordinate as:

$$\kappa = g^*K^* - gK = (g + 2\varepsilon_{11})(K + \chi_s) - gK \approx g\chi_s + 2K\varepsilon_{11}. \tag{C11}$$

The insertion of Eq. (C8) into (C11) returns $\kappa=g\chi$, which was to be demonstrated.

Appendix D

Closed-form solutions for the elements of the basic stiffness matrix of a big-curvature circular beam with rectangular cross sections are:

$$
\begin{aligned}
k_{11} &= \frac{B}{RD}\Big[2h\big(\sin\xi_k-\sin\xi_i\big)^2-2A\Delta\xi\big(\Delta\xi+\cos\xi_k\sin\xi_k-\cos\xi_i\sin\xi_i\big)\Big],\\
k_{12} &= \frac{2B}{RD}\Big\{\cos\Big[\big(3\xi_k+\xi_i\big)/2\Big]-\cos\Big[\big(\xi_k+3\xi_i\big)/2\Big]\Big\}\big(-A\Delta\xi\cos(\Delta\xi/2)+h\sin(\Delta\xi/2)\big),\\
k_{13} &= \frac{B}{D}\Big\{-A\Delta\xi\big(\cos(2\Delta\xi)-\cos\xi_i+2\Delta\xi\sin\xi_i\big)+\\
&\quad +h\Big[-\Delta\xi\big(\cos\xi_k-\cos\xi_i\big)+2\sin^2(\Delta\xi/2)\big(\sin\xi_i-3\sin\xi_k\big)\Big]\Big\},\\
k_{22} &= \frac{B}{RD}\Big\{2h\big(\cos\xi_k-\cos\xi_i\big)^2+A\Delta\xi\Big[\sin(2\xi_k)-2\big(\Delta t+\cos\xi_i\sin\xi_i\big)\Big]\Big\},\\
k_{23} &= \frac{B}{D}\Big\{2h\big(\cos\xi_i-3\cos\xi_k\big)\sin^2(\Delta\xi/2)-\\
&\quad -\Delta\xi\Big[2A\big(\Delta\xi\cos\xi_i-\cos\xi_k\sin\Delta\xi\big)+h\big(\sin\xi_i-\sin\xi_k\big)\Big]\Big\},\\
k_{33} &= -\frac{BR}{4D}\Big\langle h\Big[2\Delta\xi^2+16\cos\Delta\xi-7\cos(2\Delta\xi)-9\Big]+4\Delta\xi\Big\{A\big[2\Delta\xi-\sin(2\Delta\xi)\big]-2h\sin\Delta\xi\Big\}\Big\rangle,
\end{aligned}
\tag{D1}
$$

where:

$$
\begin{aligned}
&A = R\,\mathrm{arcoth}(2R/h),\\
&B = Eb\big(h-2A\big),\\
&D = \big(\Delta\xi-\sin\Delta\xi\big)\big[2h\big(\cos\Delta\xi-1\big)+A\Delta\xi\big(\Delta\xi+\sin\Delta\xi\big)\big],\\
&\Delta\xi = \xi_k-\xi_i.
\end{aligned}
\tag{D2}
$$

Literature

[1] V. Slivker, Foundations of Engineering Mechanics, V. Babitsky and J. Wittenburg, Eds., Springer, 2007.

[2] G. Radenković and A. Borković, "Linear Static Isogeometric Analysis of an Arbitrarily Curved Spatial Bernoulli-Euler Beam," *Comput Methods Appl Mech Eng,* vol. 341, pp. 360-396, 2018.

[3] A. Borković, S. Kovačević, G. Radenković, S. Milovanović and M. Guzijan-Dilber, "Rotation-free isogeometric analysis of an arbitrarily curved plane Bernoulli-Euler beam," *Comput Methods Appl Mech Eng,* vol. 334, pp. 238-267, 2018.

[4] A. Borković, S. Kovačević, G. Radenković, S. Milovanović and D. Majstorović, "Rotation-free isogeometric dynamic analysis of an arbitrarily curved plane Bernoulli-Euler beam," *Eng Struct,* vol. 181, pp. 192-215, 2019.

[5] A. Cazzani, M. Malagu, E. Turco and F. Stochino, "Constitutive models for strongly curved beams in the frame of isogeometric analysis," *Math Mech Solids,* vol. 21, no. 2, pp. 189-209, 2016.

[6] E. Dill, "Kirchhoff's theory of rods," *Arch Hist Exact Sci,* vol. 44, no. 1, pp. 1-23, 1992.

[7] J. Ericksen and C. Truesdell, "Exact theory of stress and strain in rods and shells," *Arch Ration Mech Anal,* vol. 1, no. 1, pp. 295-323, 1957.

[8] K. Washizu, "Some Considerations on a Naturally Curved and Twisted Slender Beam," *Journal of Mathematics and Physics,* vol. 43, no. 1-4, pp. 111-116, 1964.

[9] O. Fettahlioglu and J. Mayers, "Consistent Treatment of Extensional Deformations for the Bending of Arches, Curved Beams and Rings," *J. Pressure Vessel Technol,* vol. 99, no. 1, pp. 2-11, 1977.

[10] Z. Bažant, "Conjugate analogy for space structures," *Journal of Structural Division,* vol. 92, no. 3, pp. 137-159, 1966.

[11] M. Farshad and B. Tabarrok, "On generalized conjugate analogy for spatial rods," *Int J Mech Sci,* vol. 18, no. 11-12, pp. 525-528, 1976.

[12] M. Arici, "Reciprocal Conjugate Method for Space Curved Bars," *J Struct Eng-ASCE,* vol. 115, no. 3, pp. 560-575, 1989.

[13] Z. Li-li and Z. Yiang-hua, "Exact solution for warping of spatial curved beams in natural coordinates," *App Math Mech,* vol. 29, no. 7, pp. 933-941, 2008.

[14] A. Yu, M. Fang and X. Ma, "Theoretical research on naturally curved and twisted beams under complicated loads," *Comput Struct,* vol. 80, no. 32, pp. 2529-2536, 2002.

[15] L. Gimena, F. Gimena and P. Gonzaga, "Structural analysis of a curved beam element defined in global coordinates," *Eng Struct,* vol. 30, 2008.

[16] F. Gimena, P. Gonzaga and L. Gimena, "Stiffness and transfer matrices of a non-naturally curved 3D-beam element," *Eng Struct,* vol. 30, p. 1770–1781, 2008.

[17] F. Gimena, P. Gonzaga and L. Gimena, "Analytical formulation and solution of arches defined in global coordinates," *Eng Struct,* vol. 60, pp. 189-198, 2014.

[18] K. Lin and S. Huang, "Static Closed-Form Solutions for In-Plane Thick Curved Beams with Variable Curvatures," *J Solid Mech Mater Eng,* vol. 1, no. 8, pp. 1026-1034, 2007.

[19] K. Lin and S. Huang, "Static Closed-form Solutions for In-plane Shear Deformable Curved Beams with Variable Curvatures," *J Solid Mech Mater Eng,* vol. 1, no. 11, pp. 1362-1373, 2007.

[20] K. Lin and C. Hsieh, "The closed form general solutions of 2-D curved laminated beams of variable curvatures," *Compos Struct,* vol. 79, pp. 606-618, 2007.

[21] A. Lure, Three Dimensional Problems of the Theory of Elasticity, New York: Interscience, 1964.

[22] L. Trabucho and J. Viano, "Mathematical Modelling or Rods," in *Handbook of numerical analysis, Vol. IV*, Elsevier Science B.V., 1996, pp. 487-965.

[23] M. Jurak and J. Tambača, "Derivation and justification of a curved rod model," *Math Models Methods Appl Sci,* vol. 9, no. 7, pp. 991-1014, 1999.

[24] M. Jurak and J. Tambača, "Linear curved rod model: general curve," *Math Models Methods Appl Sci,* vol. 11, no. 7, pp. 1237-1252, 2001.

[25] J. Tambača, "A numerical method for solving the curved rod model," *Z Angew Math Mech,* vol. 86, pp. 210-221, 2006.

[26] J. Sanchez-Hubert and E. Sanchez Palencia, "Statics of curved rods on account of torsion and flexion," *Eur J Mech A Solids,* vol. 18, no. 3, pp. 365-390, 1999.

[27] T.-M. Wang and T. Merrill, "Stiffness Coefficients of Noncircular Curved Beams," *J Struct Eng-ASCE,* vol. 114, no. 7, pp. 1689-1699, 1988.

[28] A. Saleeb and T. Chang, "On the hybrid-mixed formulation of C0 curved beam elements," *CComput Methods Appl Mech Eng,* vol. 60, no. 1, pp. 95-121, 1987.

[29] A. Bendetti and A. Tralli, "A new hybrid F.E. model for arbitrarily curved beam - I. Linear analysis," *Computers & Structures,* vol. 33, no. 6, pp. 1437-1449, 1989.

[30] S. Krenk, "A general format for curved and non-homogeneous beam elements," *Comput Struct,* vol. 50, no. 4, pp. 449-454, 1994.

[31] Z. Friedman and J. Kosmatka, "An accurate two-node finite element for shear deformable curved beams," *Int J Numer Methods Eng,* vol. 41, no. 3, pp. 473-498, 1998.

[32] A. Shahba, R. Attarnejad, S. Jandaghi Semnani and H. Honarvar Gheitanbaf, "New shape functions for non-uniform curved Timoshenko beams with arbitrarily varying curvature using basic displacement functions," *Meccanica,* vol. 48, no. 1, pp. 159-174, 2013.

[33] L. Molari and F. Ubertini, "A flexibility-based finite element for linear analysis of arbitrarily curved arches," *Int J Numer Methods Eng,* vol. 65, pp. 1333-1353, 2006.

[34] V. Haktanir, "The complementary functions method for the element stiffness matrix of arbitrary spatial bars of helicoidal axes," *Int J Numer Methods Eng,* vol. 38, no. 6, pp. 1031-1056, 1995.

[35] I. Dayyani, M. Friswell and E. Saavedra Flores, "A general super element for a curved beam," *Int J Solids Struct,* vol. 51, no. 17, pp. 2931-2939, 2014.

[36] E. Marino, J. Kiendl and L. De Lorenzis, "Explicit isogeometric collocation for the dynamics of three-dimensional beams undergoing finite motions," *Comput Methods Appl Mech Eng,* vol. 343, pp. 530-549, 2019.

[37] F. Maurin, F. Greco, S. Dedoncker and W. Desmet, "Isogeometric analysis for nonlinear planar Kirchhoff rods: Weighted residual formulation and collocation of the strong form," *Comput Methods Appl Mech Eng,* vol. 340, pp. 1023-1043, 2018.

[38] E. Marino, "Locking-free isogeometric collocation formulation for three-dimensional geometrically exact shear-deformable beams with arbitrary initial curvature," *Comput Methods Appl Mech Eng,* vol. 324, pp. 546-572, 2017.

[39] A. Bauer, M. Breitenberger, B. Philipp, R. Wüchner and K.-U. Bletzinger, "Nonlinear isogeometric spatial Bernoulli beam," *Comput Methods Appl Mech Eng,* vol. 303, pp. 101-127, 2016.

[40] E. Marino, "Isogeometric collocation for three-dimensional geometrically exact shear-deformable beams," *Comput Methods Appl Mech Eng,* vol. 307, pp. 383-410, 2016.

[41] L. Greco and M. Cuomo, "B-Spline interpolation of Kirchhoff-Love space rods," *Comput Methods Appl Mech Eng,* vol. 256, pp. 251-269, April 2013.

[42] S. Timoshenko and J. Gere, Theory of elastic stability, New York: McGraw-Hill, 1961.

[43] J. Cottrell, T. Hughes and Y. Bazilevs, Isogeometric analysis: Toward integration of CAD and FEA, Chichester: Wiley, 2009.

[44] J. Gil, "On the arc length parameterization problem," *Int J Pure Appl Math,* vol. 31, no. 3, pp. 401-419, 2006.